END
DATE
FILMED

8—79

DDC

MICROCOPY RESOLUTION TEST CHART
NATIONAL BUREAU OF STANDARDS-1963-A
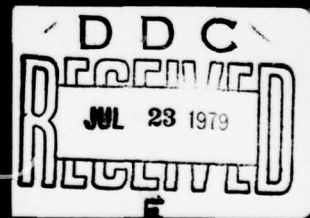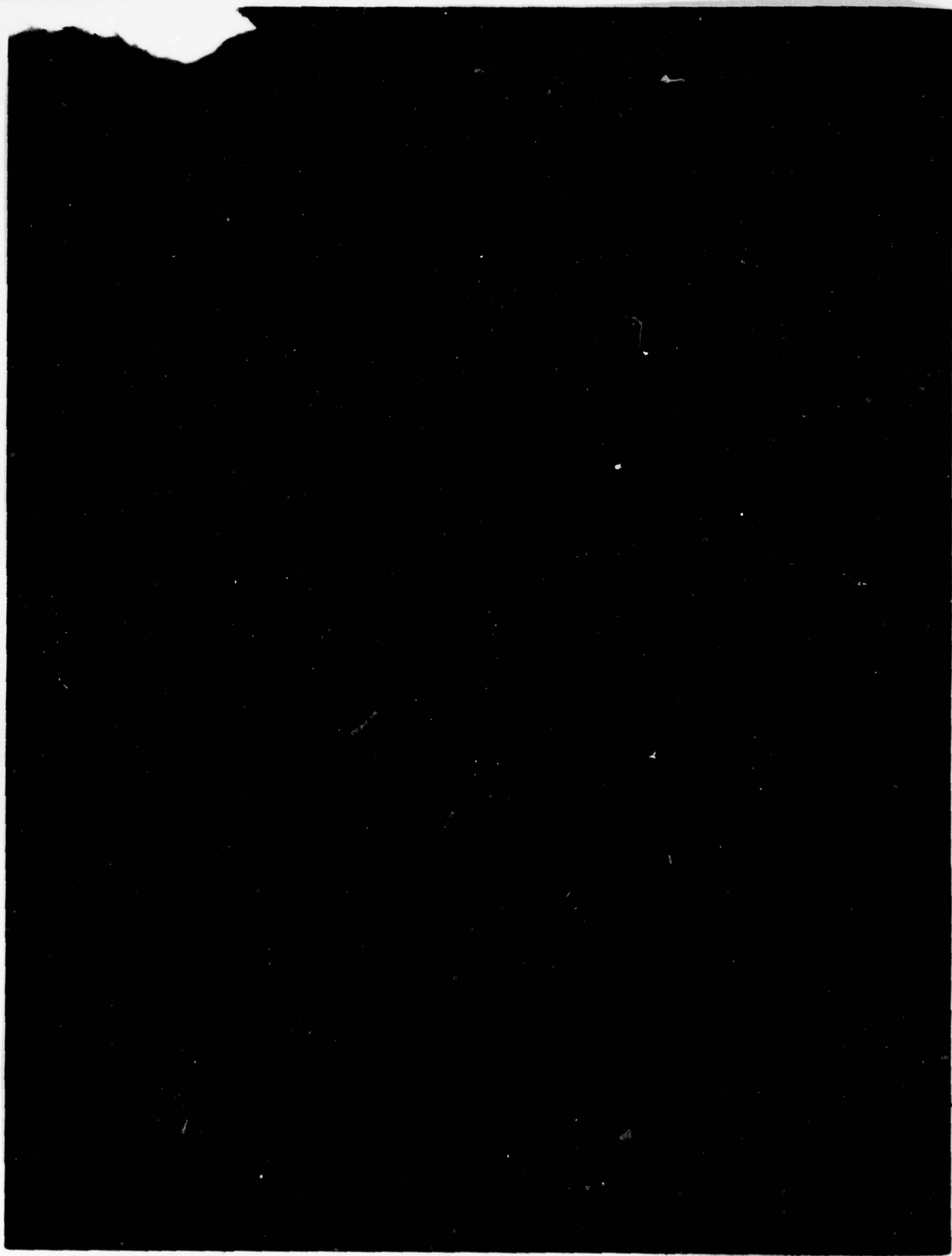
REPORT DOCUMENTATION PAGE		READ INSTRUCTIONS BEFORE COMPLETING FORM
1. REPORT NUMBER ARCSL-TR-79013	2. GOVT ACCESSION NO.	3. RECIPIENT'S CATALOG NUMBER
4. TITLE (and Subtitle) FINAL REPORT: INFRARED ABSORPTION BY WATER CLUSTERS		5. TYPE OF REPORT & PERIOD COVERED Technical Report August 1976 - September 1978
		6. PERFORMING ORG. REPORT NUMBER
7. AUTHOR(s) Hugh R. Carlon		8. CONTRACT OR GRANT NUMBER(s)
9. PERFORMING ORGANIZATION NAME AND ADDRESS Commander/Director, Chemical Systems Laboratory Attn: DRDAR-CLB-PO Aberdeen Proving Ground, Maryland 21010		10. PROGRAM ELEMENT, PROJECT, TASK AREA & WORK UNIT NUMBERS A91A
11. CONTROLLING OFFICE NAME AND ADDRESS Commander/Director, Chemical Systems Laboratory Attn: DRDAR-CLJ-R Aberdeen Proving Ground, Maryland 21010		12. REPORT DATE March 1979
		13. NUMBER OF PAGES 49
14. MONITORING AGENCY NAME & ADDRESS(if different from Controlling Office)		15. SECURITY CLASS. (of this report) UNCLASSIFIED
		15a. DECLASSIFICATION/DOWNGRADING SCHEDULE NA

16. DISTRIBUTION STATEMENT (of this Report)

Approved for public release; distribution unlimited.

17. DISTRIBUTION STATEMENT (of the abstract entered in Block 20, if different from Report)

18. SUPPLEMENTARY NOTES

19. KEY WORDS (Continue on reverse side if necessary and identify by block number)

(U)

Dimer	Ion hydrates	Emission/Adsorption
Ion product	Water clusters	Electrical conductivity
Moist air	Cluster models	Infrared absorption spectra
Water vapor	Hydrogen bonds	Infrared "continuum" absorption
Ion clusters	Polymolecular clusters	Atmospheric infrared absorption

20. ABSTRACT (Continue on reverse side if necessary and identify by block number)

(U) This report summarizes the results of a two-year study of atmospheric infrared "continuum" absorption attributed to intermolecularly bonded clusters in water vapor. Spectral data are reviewed for water vapor, steam and liquid water. The infrared continuum absorption is discussed in detail and is shown to be explicable on the basis of homogeneous or ion-induced cluster distributions in water vapor, where the cluster population is approximately proportional to the square of the partial water vapor pressure. Thermodynamic consistency between the vapor and liquid phases is discussed for temperatures including the critical (374°C) where the phases become one. Simple oscillator models are shown to give agreement with observed spectral lines, suggesting certain cluster configurations. The ion concentration of moist air versus temperature is discussed.

(continued on reverse side)

DD FORM 1473 1 JAN 73 EDITION OF 1 NOV 65 IS OBSOLETE

20. ABSTRACT. (Continued)

and measurements of ion cluster distributions are considered. Cluster absorption at longer wavelengths including the microwave region is discussed. Conclusions are presented.

SUMMARY

This report does not follow the usual research report format, because much of the experimental work performed under this effort already has been reported or published elsewhere and is included in the references. The purpose of the present report is to discuss, in a logical sequence, the present state of knowledge of atmospheric water clusters and their spectral absorption in the infrared, and at longer wavelengths. The recent work performed at the Chemical Systems Laboratory has been combined with that of other workers to give a comprehensive overview of the entire subject.

The introductory sections present and discuss spectral data for water vapor, steam and liquid water. Cluster models and expected vibrational frequencies are discussed next. Water cluster formation mechanisms are then considered for three kinds of clusters: homogeneous (like the dimer), ion clusters (ion hydrates) and ion-induced neutral clusters. Measurements of the ion content of moist air are reviewed. Cluster absorption at longer wavelengths is discussed briefly. Conclusions are drawn from the combined results of these investigations.

PREFACE

The work described in this report was authorized under In-House Laboratory Independent Research (ILIR). This work was started in August 1976 and completed in September 1978.

Reproduction of this document in whole or in part is prohibited except with permission of the Commander/Director, Chemical Systems Laboratory, Attn: DRDAR-CLJ-R, Aberdeen Proving Ground, Maryland 21010; however, DDC and the National Technical Information Service are authorized to reproduce the document for United States Government purposes.
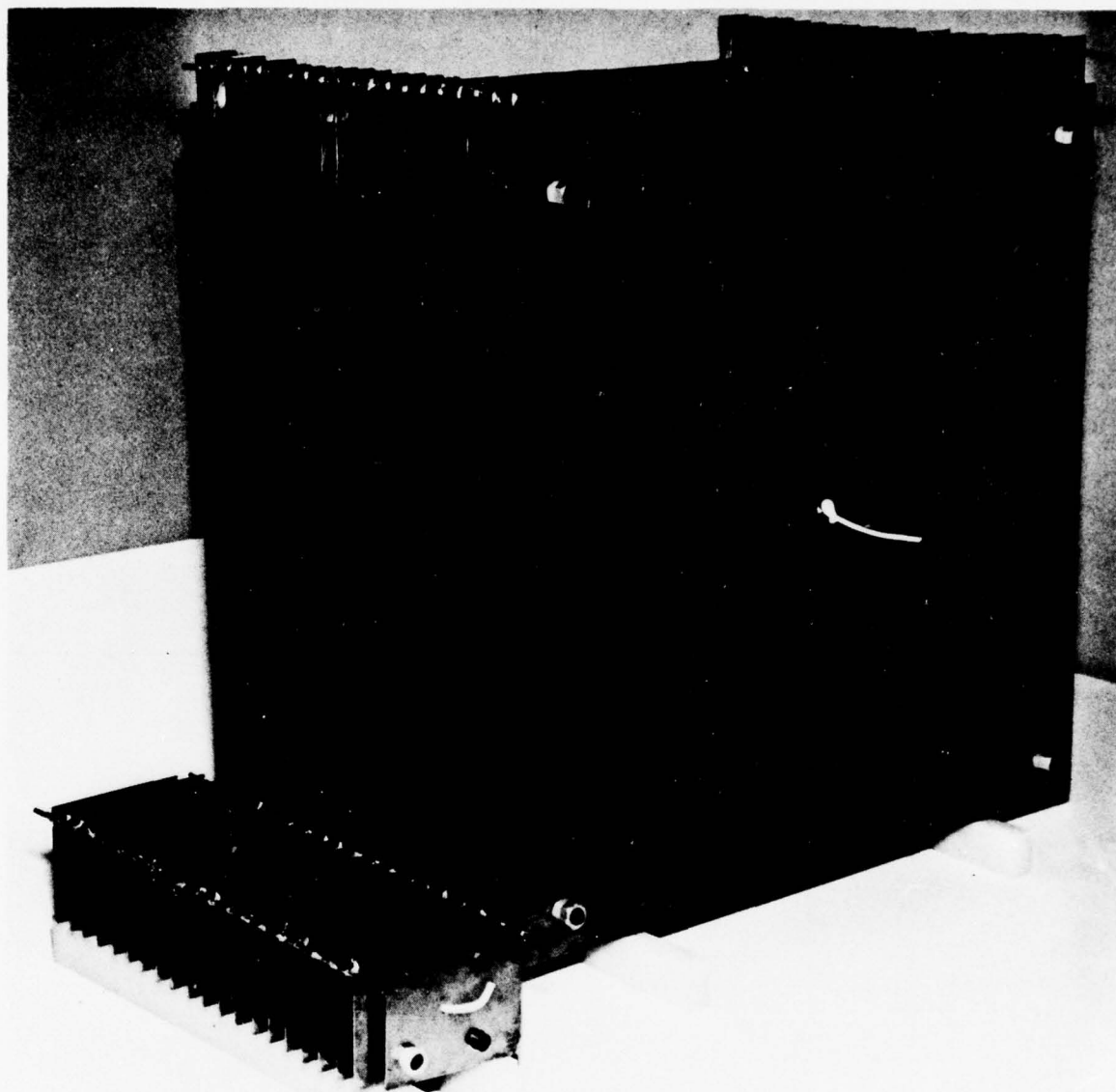
Frontispiece

Electrical Conductivity Cells Constructed for the Determination of
the Ion Content of Moist Air

CONTENTS

LIST OF FIGURES

I. INTRODUCTION.

The infrared transmission of the atmosphere is determined primarily by the transmission spectra of two gases: carbon dioxide and water vapor. The spectrum of water vapor is shown in figure 1.
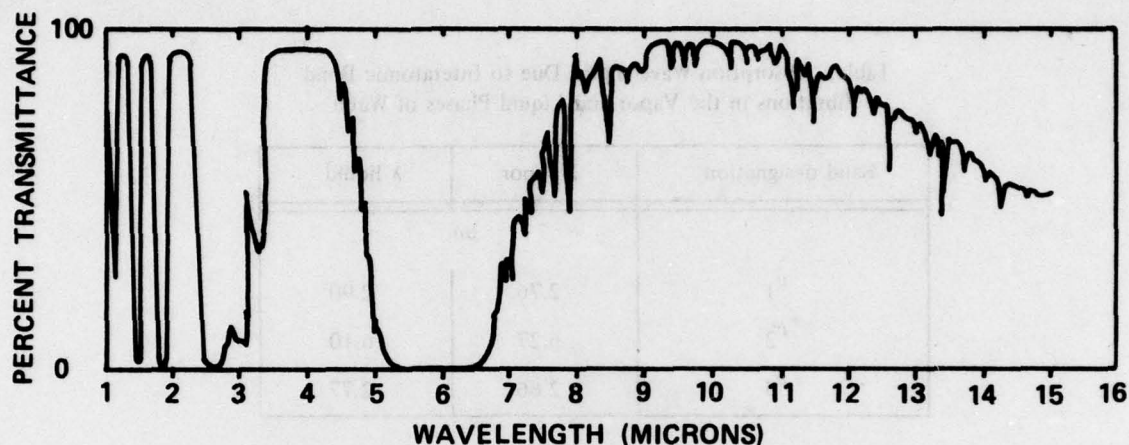
Figure 1. Infrared Transmittance of Water Vapor

Two regions of high transparency, often called "atmospheric windows", are well defined at 3-5 μm and at 8-13 μm, with strong water vapor absorption at most other wavelengths. Infrared hardware for most applications must be designed to work in one of these windows. Thus, on the one hand water vapor defines the wavelengths of hardware operation, while on the other hand it frequently limits systems performance due to complex effects which only recently are becoming understood.

There are many examples of infrared hardware systems that operate in, or on the edges of, the 3-5 μm and 8-13 μm, windows. Thermal night viewers are operable in both windows, and at 8-13 μm they have the advantage that the blackbody radiation peak falls there for objects at normal ambient temperatures. Many earth satellite experiments operate in these wavelength regions, measuring such things as temperatures of the air or of the earth's surface, humidity, and surface emissivity or reflectivity. High-powered lasers, such as the CO_2 laser at 10.6 μm, depend for application upon the transparency of the atmosphere at their operating wavelengths.

II. MOLECULAR CLUSTERING IN WATER.

For a long time it was believed that the atmospheric absorption spectrum of water in the infrared could be explained by the "vapor" only – that is, by the interatomic vibrations of individual water molecules (figure 2). These molecules have (3N - 6) or 3 vibrational modes,

11

where N is the number of atoms per molecule. These vibrations result in infrared absorption bands which are centered on several wavelengths, some of which are summarized in the table. Note that there is very little shift in these absorbed wavelengths between the vapor and liquid phases of water.
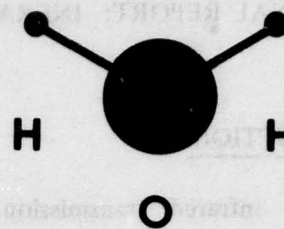
Figure 2. The Water Molecule

Table. Absorption Wavelengths Due to Interatomic Bond Vibrations in the Vapor and Liquid Phases of Water

Band designation	λ vapor	λ liquid
	μm	
ν_1	2.76	2.90
ν_2	6.27	6.10
ν_3	2.66	2.77

The spectrum of liquid water is shown in figure 3. Except for small absorption dips near 5 μm and 15 μm, it is not very different qualitatively from the spectrum of water vapor (figure 1). The large, broad absorptions due to interatomic vibrations (see table) are readily observed. But there is convincing evidence that, quantitatively, the vapor and liquid phases of water have very different infrared spectral activities.

MICRONS
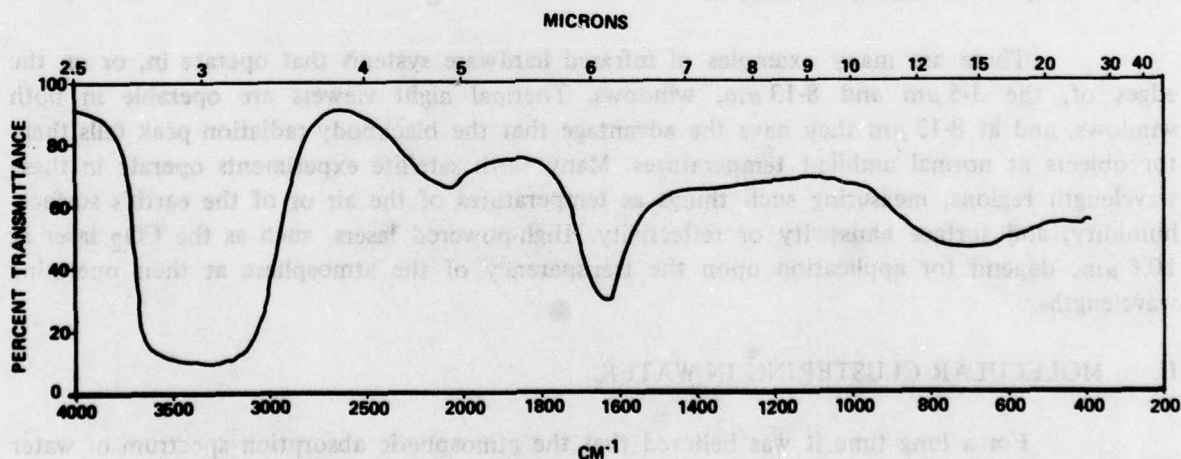
Figure 3. Infrared Transmittance of Liquid Water

In 1965, the author reported[1] that in the 8-13 μm wavelength region equal numbers of water molecules can have infrared absorptions which are very different. The absorption depends strongly upon the phase in which the molecules are found. For example, at the 10 μm wavelength, the molecular absorption coefficient of water vapor is only 10^{-4} to 10^{-3} that of a film of clean liquid water. It is now known that this behavior is due to the small fraction of water molecules which are intermolecularly bonded ("clustered") in typical water vapor samples, compared to those in the liquid phase, which are almost completely bonded together.[2] In liquid water, the intermolecular bonds are hydrogen bonds.

In 1966, it was noted that clusters (then assumed to be tiny liquid-like "droplets") could cause errors in atmospheric radiometry and could be important in the detection of clear-air turbulence (CAT).[3] Later, many examples of related phenomena were cited.[4]

In the visible and near-infrared wavelengths, water vapor and liquid have comparable absorption coefficients. But as wavelength increases, the ratio of liquid to vapor coefficients increases reaching values in the hundreds in the 3-5 μm window region, and 10^3 to 10^4 in the 8-13 μm region and beyond. This effect can be appreciated in figure 4, where the thicknesses of water vapor and liquid samples are shown for 50% transmission at the two wavelengths of observation — 8.2 μm in the vapor transmission window, and 15.0 μm, where liquid water has its peak infrared absorption due to intermolecular (hydrogen) bonds. This comparison illustrates the order of magnitude of the differential absorption. In figure 4, "s" is the saturation ratio or fractional relative humidity, and $(n_c)_\phi$ is the fraction of either phase which is clustered.

THESE VOLUMES CONTAIN
EQUAL NUMBERS OF
HYDROGEN BONDS

PARAMETER:	WATER VAPOR:	"PURE" LIQUID WATER:
TEMPERATURE, θ_c	30°C	30°C
SATURATION RATIO, (s)	0.25	N/A
MASS FRACTION, $(n_c)_\phi$	10^{-4}	ASSUMED 1.0
λ	8.2μm	15.0μm
PATH LENGTH (Lm)	9124m	2.06 × 10^{-6}m
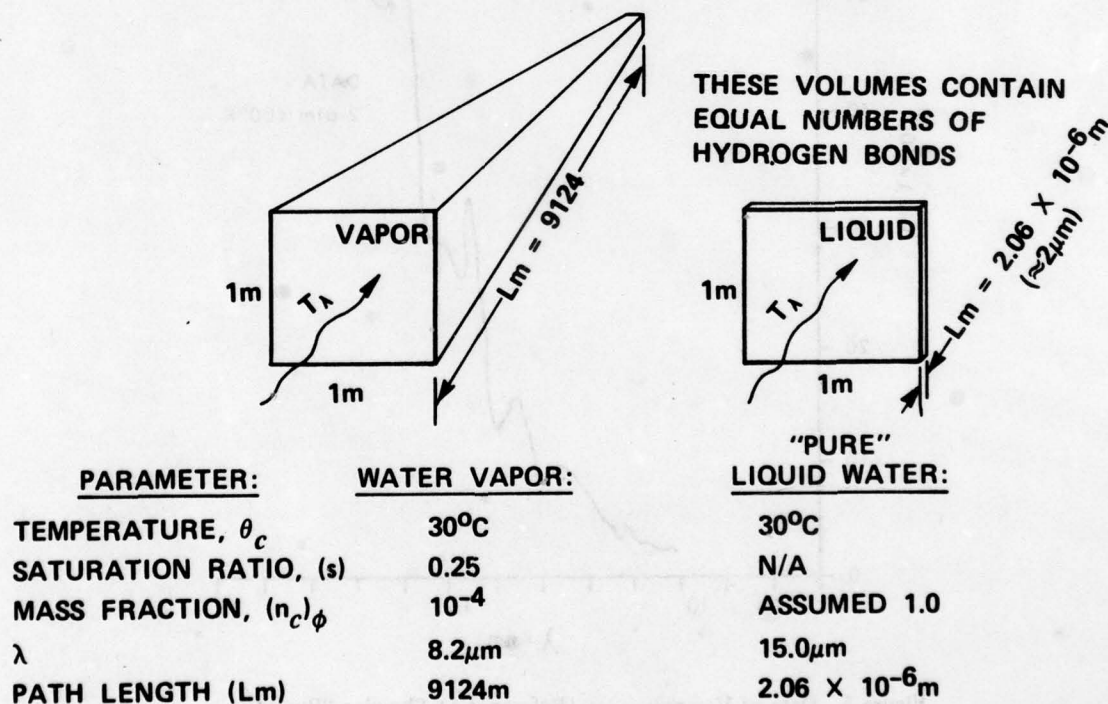
Figure 4. Comparison of Vapor and Liquid Water Samples
for Equal Absorption

It has been known for many years that a far-infrared "continuum" absorption exists in water vapor which increases with wavelength to beyond 20 μm. Until recently, attempts were made to explain this absorption using standard or modified vapor models without regard for the possible existence of other water species such as clusters.

In 1968, infrared spectra of steam were observed which had regularly spaced "bumps" (figure 5). But the main thrust of this and subsequent work has been to show that the continuum absorption not only is large, but that it has a quadratic pressure dependence, and that its absorption coefficient has a small negative temperature dependence. However, it was recognized for the first time[5] that these results were consistent with the idea that intermolecular hydrogen bonding contributes to the absorption coefficient of water "vapor" in the far infrared. In 1971, the author first examined anomalous emission spectra of steam in the 8-13 μm window region, and related the observed results to tiny "droplet" (cluster) effects at many wavelengths.[6]
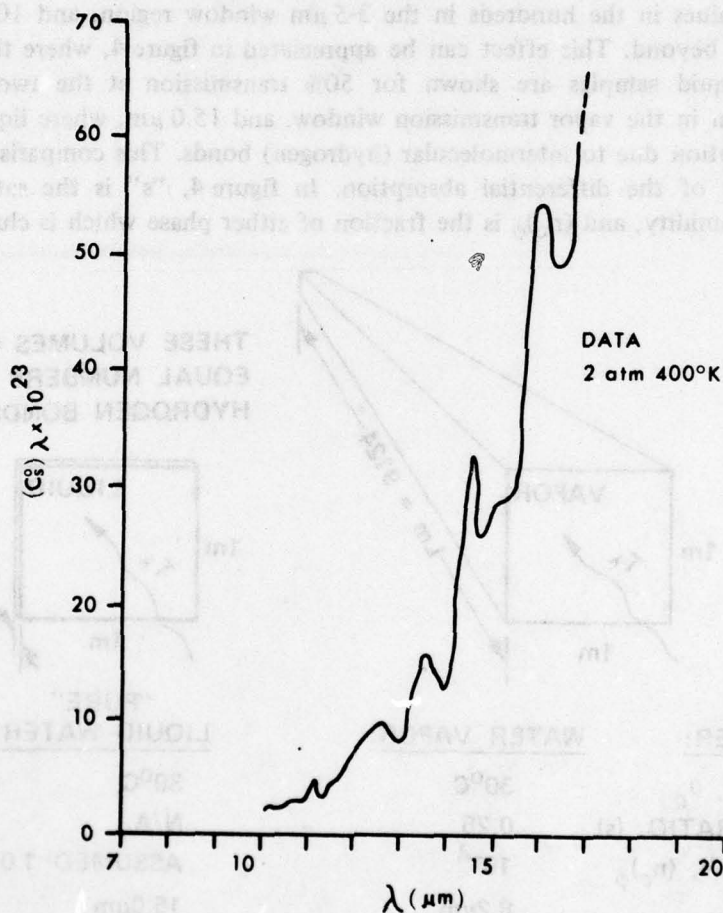
Figure 5. Data of Varanasi, *et al.* (Reference 5), Showing "Bumps"
$(C_s^0)_\lambda$ is the "continuum" absorption coefficient, in
units cm^2/molecule-atmosphere of water vapor.

14

The "dimer school" of water vapor absorption[7,8,9] was the logical outgrowth of the idea of hydrogen bonding in water vapor. It was assumed that the dimer, or hydrogen bonded cluster of size 2, was homomolecular and was an intermediary to all larger clusters. Consequently, the dimer was thought to be the most prevalent of water cluster species.

But the author's more recent measurements of the infrared emission spectra of cooling steam clouds[10] * show unusual, stepwise changes corresponding to rather small changes in cloud droplet mass concentration or temperature. Examples are shown in figure 6. These results suggest that "avalanche-like" shifts occur in the size and number distributions of clusters in water vapor, corresponding to changes in environmental parameters. The transitions are not smooth. Thus, there is evidence for more than one cluster species (the dimer) in these results and in other data to be discussed in this paper.

Spectroscopists working with liquid water and its solutions long have been aware of features in the infrared absorption spectrum of the liquid which could not be explained on the basis of simple interatomic vibrations (figure 2 and table). While clean liquid water has bands near $3 \mu m$ and $6 \mu m$ wavelengths attributable to interatomic vibrations just as the vapor spectrum does, there are bands peaking at $4.7 \mu m$ and $15.7 \mu m$ which have a different origin. Figure 7 shows the infrared absorption coefficient of clean liquid water[11] plotted over a wide spectral range. The "bump" at $4.7 \mu m$ is attributed to the hydronium ion, (H_3O^+),[12] and the huge peak at $15.7 \mu m$ is attributed to intermolecular hydrogen bonding or clustering of water molecules.[13]

Hence, liquid water can be thought of as being made up mostly of "ice-like" lattices[14] or clusters. But in water vapor, only a small fraction of water molecules are hydrogen bonded to form "liquid-like" clusters. In both phases, the nature of intermolecular bonding is similar. The cluster configurations determine the vibrational frequencies or resonant wavelengths of particular bonds, and thus their infrared absorption line spectra. The resulting infrared line or band strengths will depend, first, upon the frequency or wavelength of absorption for given bonds in given cluster configurations and, second, upon the numbers of each configuration which are present in the cluster distribution.

III. THE "CONTINUUM" ABSORPTION.

It is instructive to look at the continuum absorption of water "vapor", for clues as to the numbers and kinds of water clusters found in water vapor or in moist air, and their relationships to humidity and temperature.

Figures 8 a. and 8 b. show the infrared continuum absorption,[15] attributed here to intermolecular bonding between water molecules in the vapor phase. Continuum absorption by water vapor also exists in the $3-5 \mu m$ wavelength region, where it is ten to twenty times weaker than at $10 \mu m$.
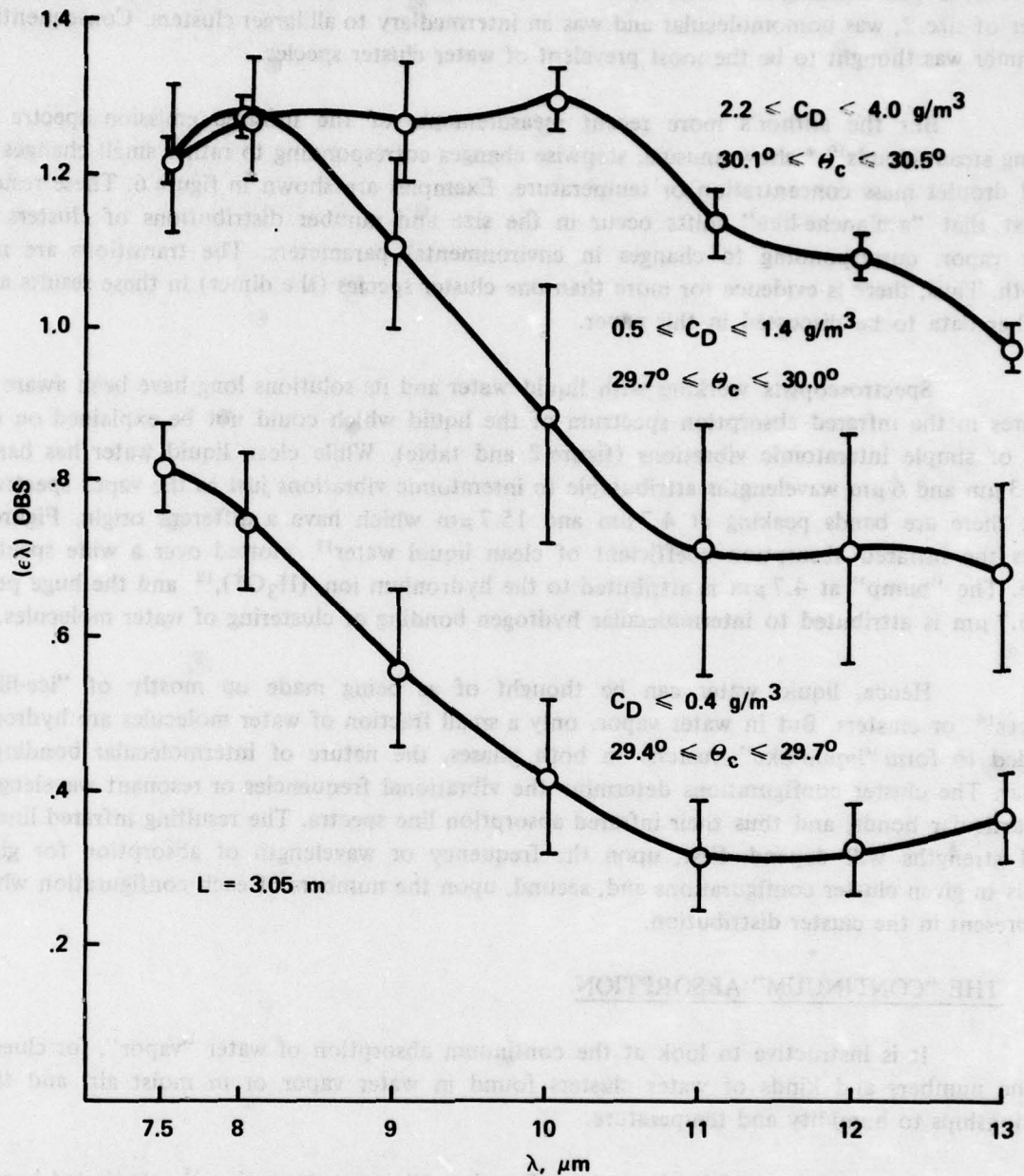
Figure 6. Typical Data from Carlon, Unpublished Paper, Showing Changes in Warm Water Cloud Emissivity

$[(\epsilon_\lambda)_{obs}$, with changes in droplet mass (volume) concentration, C_D, gm/m^3. θ_c is the cloud temperature in Celsius, and L is the optical path length, 3.05 m.]
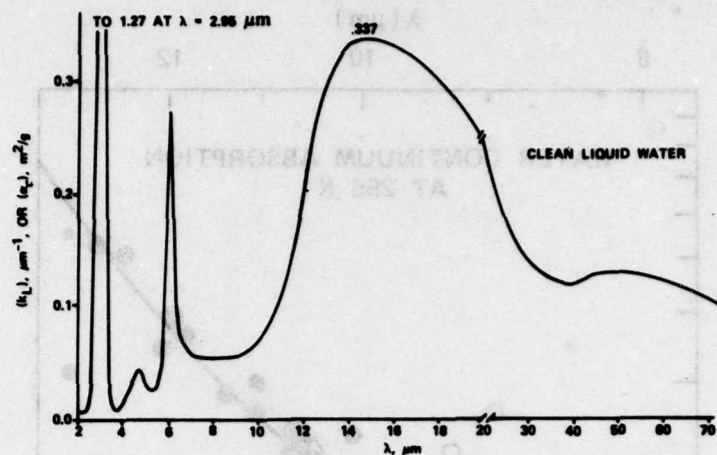
Figure 7. Absorption Coefficient Spectrum for Liquid Water
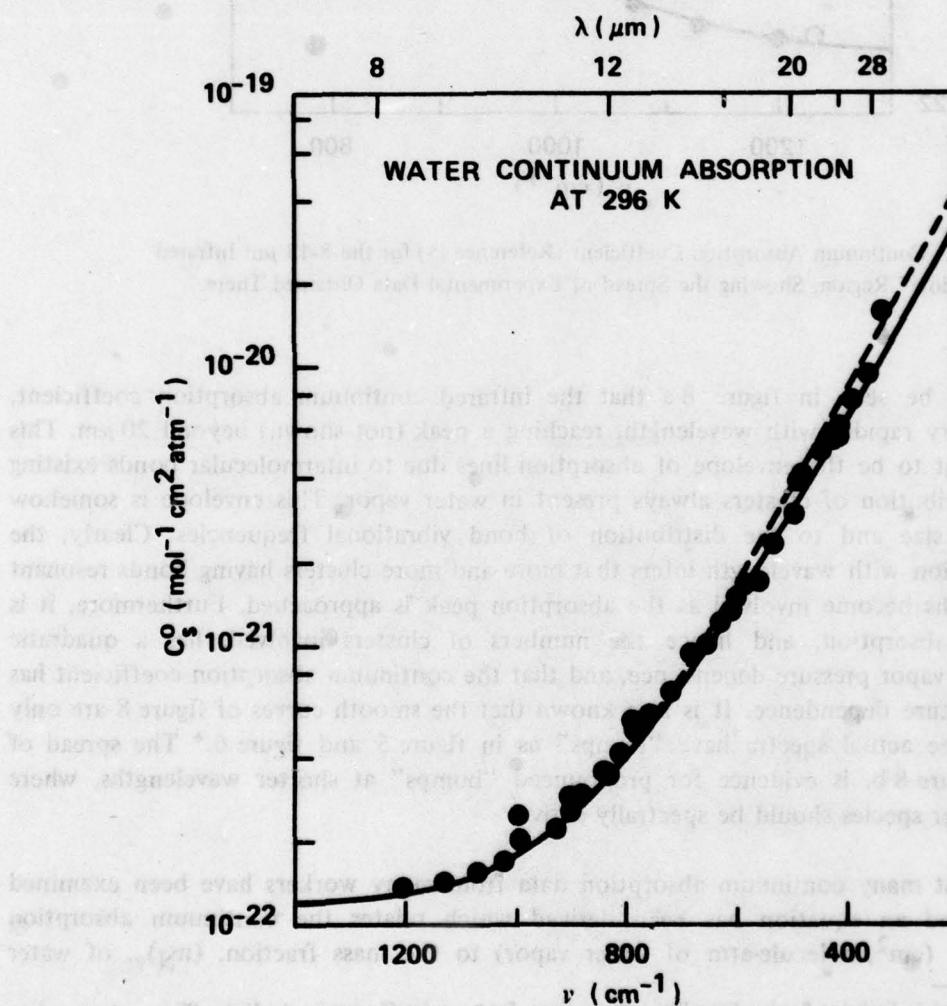
Figure 8 a. Continuum Absorption Coefficient (Reference 15) for the 8-30 μm
Infrared Wavelength Interval
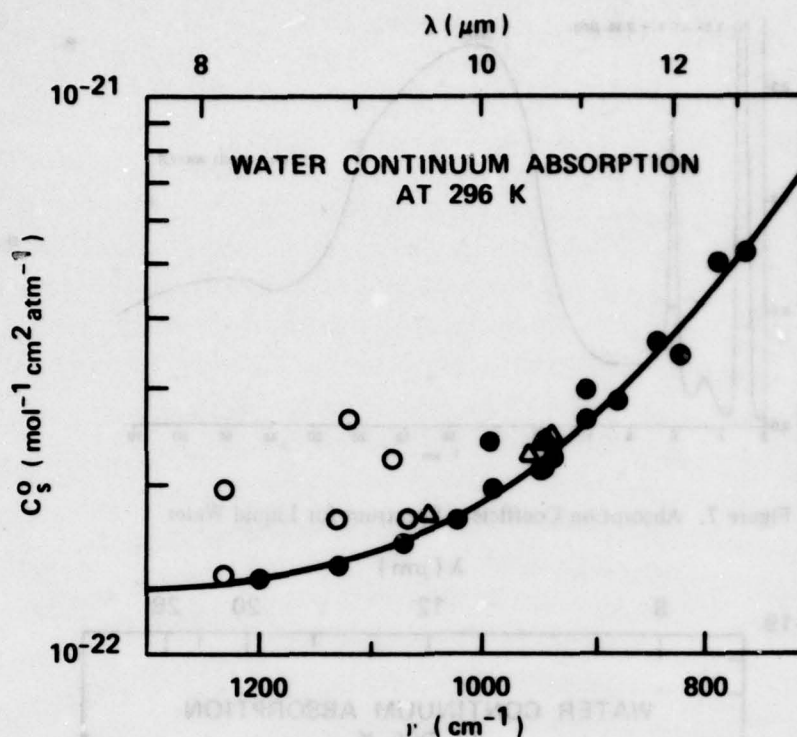
Figure 8 b. Continuum Absorption Coefficient (Reference 15) for the 8-13 μm Infrared "Window" Region, Showing the Spread of Experimental Data Obtained There

It can be seen in figure 8 a that the infrared continuum absorption coefficient, $(C_s^o)_\lambda$, increases very rapidly with wavelength, reaching a peak (not shown) beyond 20 μm. This spectrum is thought to be the envelope of absorption lines due to intermolecular bonds existing in the typical distribution of clusters always present in water vapor. This envelope is somehow related to cluster size and to the distribution of bond vibrational frequencies. Clearly, the increase in absorption with wavelength infers that more and more clusters having bonds resonant at these wavelengths become involved as the absorption peak is approached. Furthermore, it is known that this absorption, and hence the numbers of clusters involved, has a quadratic (approximately s^2) vapor pressure dependence, and that the continuum absorption coefficient has a negative temperature dependence. It is also known that the smooth curves of figure 8 are only approximations. The actual spectra have "bumps" as in figure 5 and figure 6.* The spread of data points in figure 8 b. is evidence for pronounced "bumps" at shorter wavelengths, where smaller water cluster species should be spectrally active.

A great many continuum absorption data from many workers have been examined by the author, and an equation has been derived which relates the continuum absorption coefficient, $(C_s^o)_\lambda$, (cm^2/molecule-atm of water vapor) to the mass fraction, $(n_N)_v$, of water

*Carlon, H. R.   Variations in Emission Spectra from Warm Water Fogs: Evidence for Clusters in the Vapor Phase.   Accepted for publication in Infrared Physics, approximately December (1978).

18

vapor which must be clustered to account for the observed infrared continuum absorption at a given wavelength.[16] The minimum required fraction is:

$$(n_N)_V = \frac{(C_s^0)_\lambda N(s) (p_0) (n_c)_\ell}{7.6 \times 10^{-17}}$$ (1)

where N refers to the clusters which are spectrally active at wavelength λ, (p_0) is the water vapor saturation pressure at some temperature, and $(n_c)_\ell$ is the fraction of liquid water which is hydrogen bonded at that temperature (from reference 2).

In order to derive equation 1, the assumption was made that the intermolecular (hydrogen) bond absorption coefficient for vapor-phase clusters could be approximated from the peak absorption coefficient of liquid water at the $15.7 \, \mu$m wavelength (figure 7), and that the nature of clustering was at least similar in both phases so that the result could be extrapolated to vapor-phase clusters. The results indicate that these were reasonably valid assumptions.

Many continuum absorption data were substituted directly into equation 1 to yield the result that at a given temperature the *total* mass fraction of all clusters of all sizes in the distribution is given by:

$$(n_c)_V = \sum_{2}^{N} (n_N)_V = K (s)$$ (2)

That is, the result showed that the mass fraction of water vapor clustered as species responsible for the infrared continuum absorption at some wavelength is equal to the water vapor saturation ratio (s) times a constant. The actual mass concentration of these species in the vapor sample would then be the mass fraction times the vapor concentration, or:

$$C_c = (n_c)_V C_1 = \frac{(n_c)_V (k) (s) (p_0)}{\theta_k}$$ (3)

or

$$C_c = \frac{k K (s)^2 (p_0)}{\theta_k}$$ (4)

where C_c is the species concentration, gm/m^3, C_1 is the water vapor concentration, gm/m^3, k is a gas constant numerically equal to 289, K is an empirical constant from equation 2, and θ_k is the Celsius temperature.

These results show that at a given temperature, the actual concentration of species (assumed to be water clusters) responsible for the infrared continuum absorption at some wavelength is proportional to $(s)^2$. In other words, it is the concentration of these species that determines the $(s)^2$ dependency of the infrared continuum absorption.

This same analysis also gives an insight into the nature of the temperature dependence of the continuum absorption coefficient, $(C_s^0)_\lambda$.

19

In recent work at the Chemical Systems Laboratory it has been learned that the dependence of the cluster fraction upon temperature obeys a function of the Clausius-Clapeyron form:

$$\ln (n_c)_v = (C) - \frac{\Delta H}{R\theta_k} \tag{5}$$

where C is an empirical constant, ΔH is the latent heat of vaporization of water, and R is a gas constant - 1.987 gm-cal/mole-^{O}K. When C is evaluated and the equation is rewritten, it is found that the cluster fraction can be expressed as:

$$(n_c)_v = \exp \left(-1.04 - \frac{4.34\,\Delta H}{\theta_k} + \ln(s) \right) \tag{6}$$

Equation 6 has a form not unlike that obtained empirically for the temperature correction of the continuum absorption by Roberts, et al.[15] Substitution of $(n_c)_v$ from equation 6 in equation 1, with rearrangement, yields a new expression:

$$(C_s^O)_\lambda = \frac{7.6 \times 10^{-17} \exp \left(-1.04 - \frac{4.34\,\Delta H}{\theta_k}\right)}{(p_o)\,(n_c)_\ell} \tag{7}$$

Equation 7 is plotted in figure 9. The form of equation 7 agrees well with the trend of recent experimental data obtained by Montgomery.[17] Earlier measurements had included only that range of temperatures below 115°C, represented by the left-hand portion of the curve in figure 9. Thus, an empirically-obtained temperature correction such as that of Roberts, et al,[15] approximated the slope of the curve for earlier data. Similarly, attempts to assign a constant cluster bond strength or "binding energy", $(\beta)_{ev}$, lead to incorrect approximations at higher temperatures. It is the change in ΔH with temperature that accounts for the curve shape in figure 9.

The latent heat of vaporization of water, ΔH, is a fundamental thermodynamic property associated with the energy required to break or to form intermolecular bonds during the vapor/liquid phase transition. The finding that the infrared continuum absorption coefficient of water "vapor" can be simply described, as a function of temperature, by an expression containing ΔH (equation 7), therefore provides a powerful argument that the anomalous absorption is due to liquid-like water clusters in the vapor phase.

By insisting upon thermodynamic consistency of the behavior of water in both the vapor and liquid phases, up to and including the critical temperature (374°C) where these phases become one, it is possible to gain further insights into the nature of the clustering process. For example, if $(n_c)_v$ from equation 6 is plotted with the cluster fraction $(n_c)_\ell$ for liquid water[2], it is found that the clustered fractions of the two phases converge at the critical temperature. This is shown in figure 10.

Furthermore, there is evidence that the latent heat of vaporization of water consists of two components. One component includes the intermolecular forces common to all liquids, while a second (latent) component is associated with the hydrogen bonding which is peculiar to water. This, illustrated in figure 11, where ΔH is plotted as a function of the weight fraction of "O-H" in the water molecules. Pure water has a fraction of 1.0 (indicated here for the fraction of bonds that are broken-?), while nonane represents the 0.0 fraction. In between, various straight chain alcohols are represented by different fractions. It can be seen that the latent heat (which is temperature-dependent for the data represented) falls rapidly with falling hydrogen bond content of the molecule, attaining a level typical of many other substances which are not hydrogen bonded, as the weight fraction of O-H approaches zero.

Figure 10. Fraction of Water Molecules Clustered in Liquid Water (Top Curve) and Water Vapor (Lower Curve) Versus Temperature

Figure 9. Variation of $(C_3^0)_\lambda$ with Temperature from Equation 7 (Upper Curve), Compared to Data Points of Montgomery (Reference 17) [Also shown are the correction of Roberts, et al. (reference 15 dashed curve), and two curves for constant bond strengths or "binding energies" (lower curves.]

21

Furthermore, there is evidence that the latent heat of vaporization of water consists of two components. One component includes the interattractive forces common to all liquids, while a second (larger) component is associated with the hydrogen bonding which is peculiar to water. This is illustrated in figure 11, where ΔH is plotted as a function of the weight fraction of "O-H" in various molecules. Pure water has a fraction of 1.0 (corrected here for the fraction of bonds from reference 2), while nonane represents the 0.0 fraction. In between, various straight chain alcohols are represented by different fractions. It can be seen that the latent heat, ΔH (which is also temperature-dependent for the data represented) falls rapidly with falling hydrogen bond content of the molecule, attaining a level typical of many other substances which are not hydrogen bonded, as the weight fraction of O-H approaches zero.
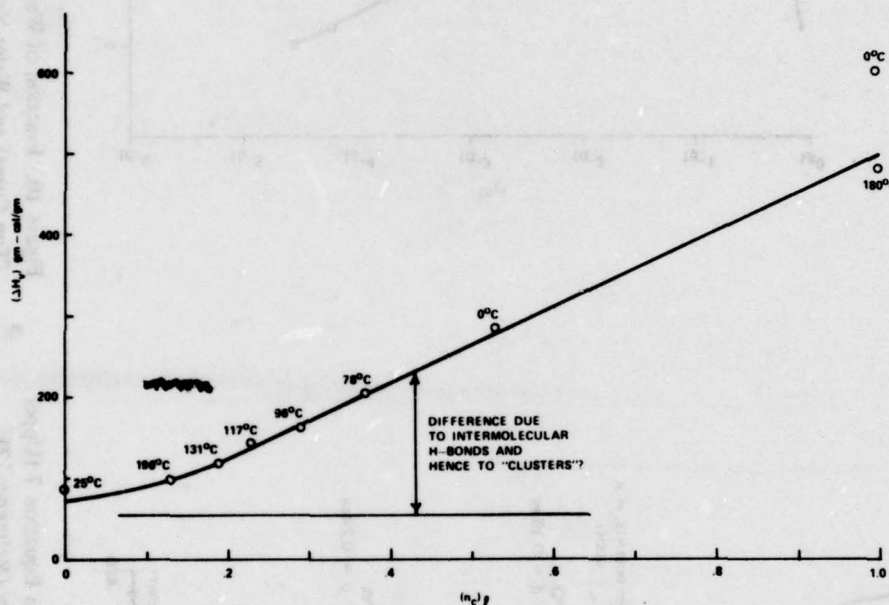
Figure 11. Latent Heat of Vaporization, ΔH, Versus Weight Fraction of "O-H" in Molecule; Liquid Water is at $(n_c)_\varrho = 1.0$

IV.   WATER CLUSTER MODELS.

Consider a simple oscillator[16] consisting of two masses connected by a bond, as in figure 12. Envision groups of water molecules "clustered" on either end of the intermolecular bond which, because of its inherent strength and the magnitude of the masses, is resonant at some wavelength, λ_c. The expression for λ_c becomes:

$$\lambda_c = 2\pi C_v \sqrt{\frac{1}{K}\left(\frac{M_1 M_2}{M_1 + M_2}\right)} \qquad (8)$$

22

where C_v is the speed of light, K is an empirical constant, and M_1 and M_2 are the masses from figure 12. M is the molecular weight of water, and n_1 and n_2 are the numbers of molecules on either side of the bond.
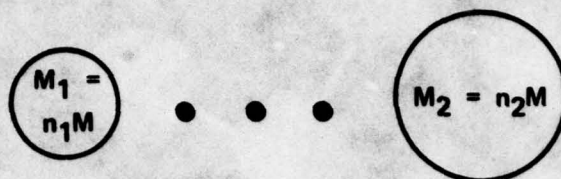
Figure 12. Simple Oscillator Model

Substitution in equation 8 gives:

$$\lambda_c = 2\pi C_v \sqrt{\frac{M}{K}\left(\frac{n_1 n_2}{n_1 + n_2}\right)} \tag{9}$$

Now consider the special case of symmetry, or equal mass on either side of a given bond. Here, $n_1 = n_2 = (c)/2$, where (c) is the "size" or number of molecules in the cluster and $(c) = n_1 + n_2$. Substitution in equation 9 yields:

$$\lambda_c = K_v \sqrt{c} \tag{10}$$

where K_v is another empirical constant. This result shows that for cluster symmetry about a given intermolecular bond, the resonant wavelength of the bond becomes a simple function of the square root of the cluster size. Exactly such a relationship was found in an examination of experimental data of many workers, for the vapor phase.[18]

From the development to this point it can be seen that if the actual vapor phase distribution of clusters by size (c) were known, and if K_v could be evaluated, in principle it should be possible to calculate an approximate infrared spectrum directly for that cluster distribution, given that the clusters were reasonably symmetrical.

Any agreement between the simple model shown here, and actual data, is surprising because equation 8 is extremely simplistic. Agreement suggests that only the simplest, most energetic cluster vibrational modes are associated with the infrared wavelengths, and that the 8-13 μm "window" lies near the extreme short-wavelength (high-frequency) end of the range of cluster spectral activity.

Several kinds of cluster configurations could have symmetrical properties. These would include straight water molecule chains, clusters in which water molecules were "swarmed" in a single layer about a central molecule or ion, and, if the cluster size were fairly large, even closed or ring structures.

For example, the open-structured cluster of figure 13 would have many modes (frequencies) associated with it. But by simple hydrogen bonding of water molecules at the extremities to form closed rings, as in figure 14, the frequencies of most bonds would be brought closer together, and the cluster would be more likely to be characterized by a fairly narrow band of absorption lines centered on some wavelength.

23
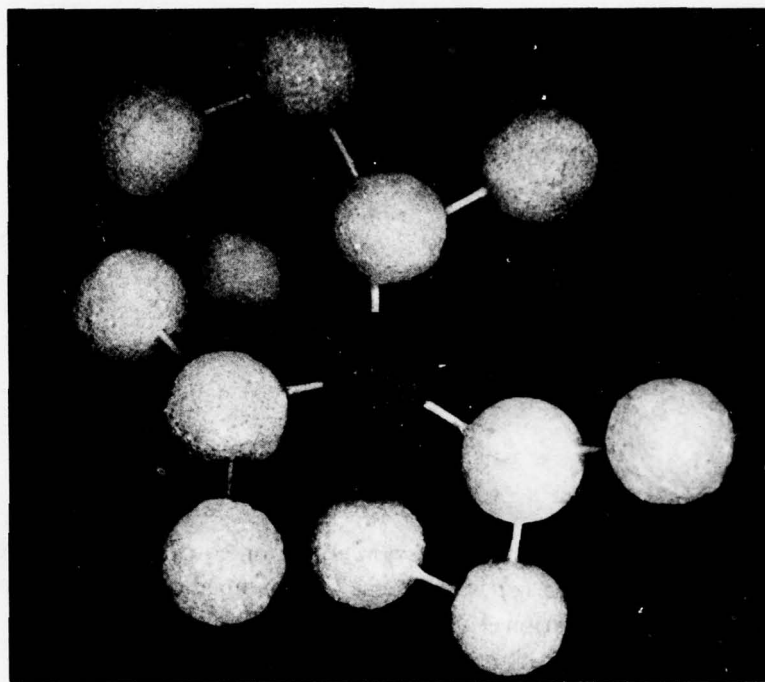
Figure 13. Open-Structured Cluster (c = 13)
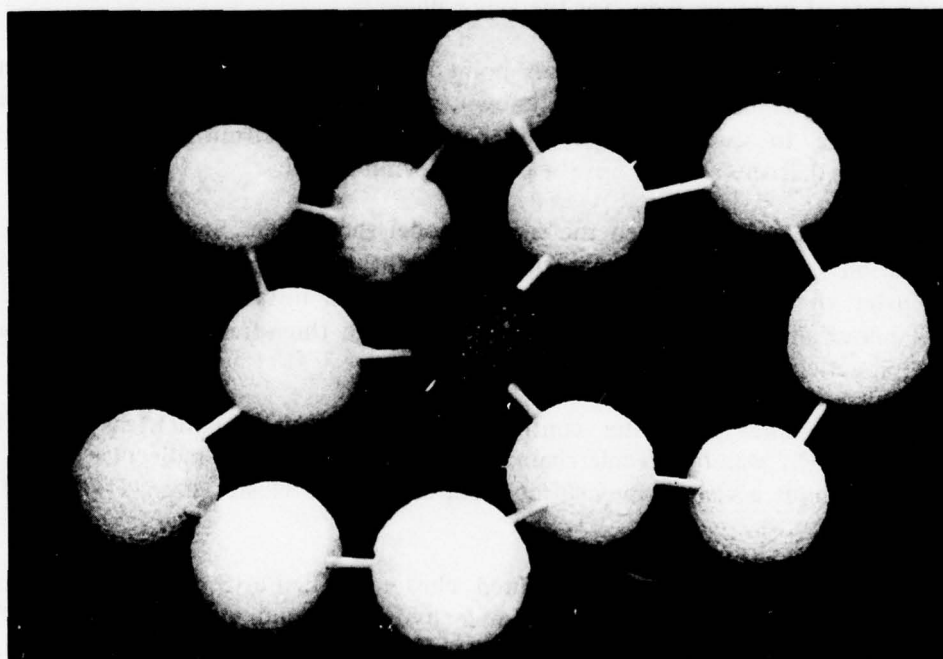
Figure 14. Closed-Ring Structure (c = 13)

24

If vapor phase water clusters can grow sufficiently large, they attain a "critical" cluster size at some supersaturation which is very dependent upon temperature. Typically, the critical cluster size for a cluster to nucleate a liquid water droplet is about (c) = 30 beginning at standard ambient conditions. Certain cluster configurations seem to be "favored". For example, the cluster in figure 14 could be considered to consist of three overlapping "hexamers", or subgroups.

It will be shown presently that the infrared absorption peak for liquid water at 15.7 μm (figure 7) can be attributed to hexamer "clusters" in the liquid phase. Thus, as a building block in cluster growth and nucleation, the hexamer has much to recommend it. It is known, for example, that water frozen into snowflakes invariably "prefers" hexagonal shapes (figure 15).
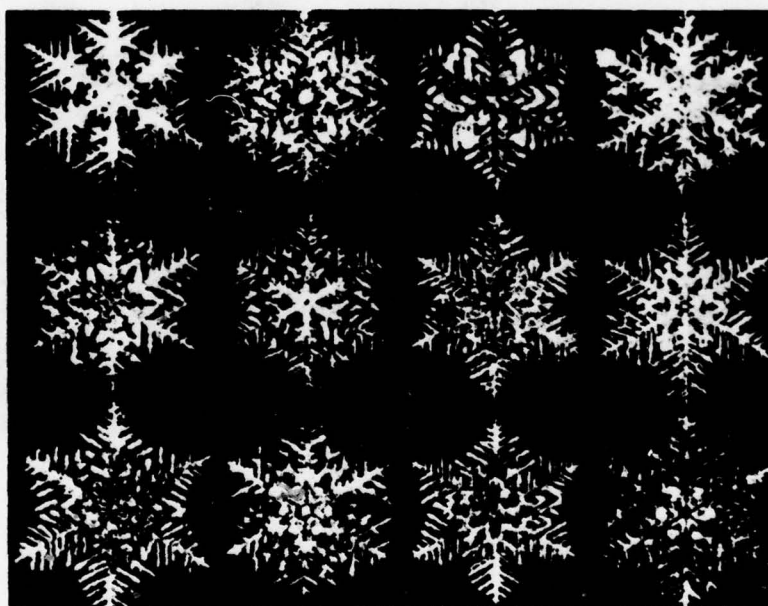
Figure 15. Hexagonal Snowflake Patterns

As cluster growth in the vapor phase progresses toward nucleation, hexamers and pentamers can combine to form "solids". The irregular, icosahedral cluster (c = 36) shown in figure 16 is also shown as a solid, where interfacial "points" represent oxygen atoms or whole water molecules, and edges represent hydrogen bonds. This cluster, in fact, would be a serious candidate for the actual structure found in liquid water. Liquid water is known to be nearly completely hydrogen bonded,[2] and to consist of "icelike" clusters[14] of a size large enough to be stable; that is, able to form the smallest possible liquid "droplets".

25
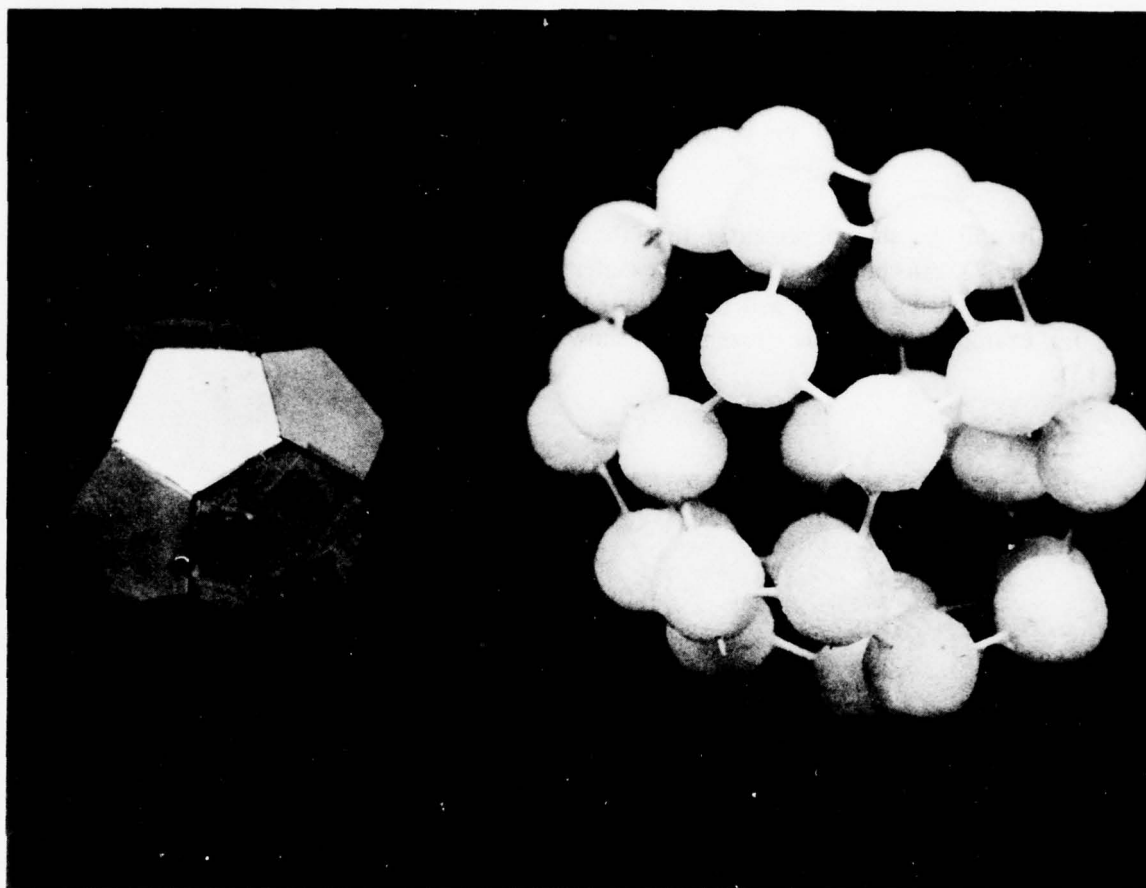
Figure 16. Irregular Icosahedral Cluster (c = 36)

V.   WATER CLUSTER FORMATION MECHANISMS.

Many uncertainties exist concerning the kinds of water clusters to which the infrared continuum absorption of water "vapor" is attributed. Rather convincing arguments can be made for each of the following kinds of clusters: (A) homogeneous clusters (example – the dimer), (B) ion clusters (ion hydrates), and (C) ion-induced, neutral clusters.

While type "A" is always assumed to be homomolecular, types "B" and "C" can be either homomolecular or heteromolecular depending upon the kinds of ions involved in the clustering processes. Each of these types or kinds of clusters will now be considered.

26

A.   Homogeneous clusters.

Homogeneous clusters form by simple, sequential reactions between water molecules which may be represented as:

$$H_2O \underset{}{\overset{+H_2O}{\rightleftharpoons}} (H_2O)_2 \underset{}{\overset{+H_2O}{\rightleftharpoons}} (H_2O)_3 \ldots \ldots \qquad (11)$$

monomer   dimer   trimer
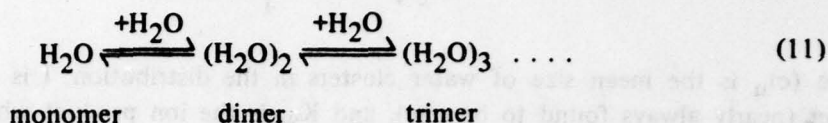
Equilibrium constants are such that the expected fraction of the dimer formed in water vapor is about 10^{-3} to 10^{-2} under standard conditions, and the fraction of each larger cluster size is about 10^{-2} that of its predecessor. Thus, expected equilibrium populations of homogeneous clusters can be represented by a distribution which decreases rapidly as cluster size increases. For example, the fractions of monomer, dimer and trimer might be about 10^{0}, 10^{-2} and 10^{-4}, respectively.

Therefore it is understandable that some workers investigating the infrared continuum absorption have consistently attributed it to the dimer.[5,7,8,9] Recent papers continue this trend, not only for data taken in the infrared,[19] but for data taken at much longer wavelengths including the microwave region.[20] Unfortunately, such a simple explanation does not account for many other kinds of observations which have been made by other workers.[*] Attempts to model anomalous water vapor absorption by Boltzmann-like distributions seem effective at lower temperatures, but break down completely at higher temperatures (see figure 9).

Thus, the dimer may be a contributor to the infrared continuum absorption of water (perhaps even an important contributor at lower temperatures). But the dimer cannot account for observed behavior at higher temperatures,[17] or for certain other observations which will be described in subsequent sections of this paper.

B.   Ion Clusters (Ion Hydrates).

It is well known that ions in water vapor cluster water molecules about themselves. Very strong arguments can be advanced to support these species as the water clusters predominantly responsible for nearly all reported observations of anomalous water vapor absorption in the infrared, and at longer wavelengths. One major discrepancy exists, however: *the numbers of ions in water vapor are far fewer than the numbers of water clusters inferred from spectral measurements.*

There is an alternative explanation which resolves this discrepancy, and this will be discussed in section V. C. The reader should bear in mind, through the lengthy discussion of ion clusters which follows, that while their behavior can be well described, their numbers simply cannot account directly for the observed spectral results.

---

[*]Carlon, H. R.   Molecular Interpretation of the ir Water Vapor Continuum: Comments, Accepted for publication in Applied Optics *17* (1978).

27

Empirical observations show that the fraction of water vapor, $(n_c)_v$, which must be clustered to account for observed infrared continuum absorption, has a very simple relationship to the ion product of water:

$$(n_c)_v = \frac{68\,(c)_u\,(s)\sqrt{K_w}}{I} \qquad (12)$$

where $(c)_u$ is the mean size of water clusters in the distribution, I is the number of ions per cluster (nearly always found to be one), and K_w is the ion product which can be obtained for any temperature from the relationship:[21]

$$K_w = \exp\left(-8.17 - \frac{7156}{\theta_k}\right) \qquad (13)$$

The form of equation 13 is not unlike that of equation 6. There are several possible explanations for this functional dependency of the cluster fraction on the ion product. The ion product is an equilibrium property of water, like the latent heat of vaporization is, and both can be reproduced in careful measurements as functions of temperature. Thus, the ability to express $(n_c)_v$ reproducibly as a function of the ion product may simply reflect the equilibrium dependencies of both upon water vapor temperature.

Another possibility is that the apparent dependence of $(n_c)_v$ on $\sqrt{K_w}$ exists (especially at higher temperatures) because dissociative ions of water can, themselves, serve as ionic "nuclei" for the formation of ion clusters of a homogeneous kind. There is considerable evidence that this behavior occurs, for example, in superheated steam.

The "reaction" for the formation of ion clusters (ion hydrates) can be written:

$$I^{\pm} + n\cdot(H_2O) \longrightarrow (I^{\pm})(H_2O)_n \qquad (14)$$
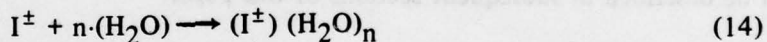
The process by which ion clusters form is shown rather simplistically in figure 17 for clusters of size $c = 4$. A positive or a negative ion appears in water vapor, and immediately attracts many monomers to itself. The oxygen atoms of the monomers orient themselves toward positive ions, and the hydrogen atoms of the monomers orient themselves toward negative ions. Almost immediately, hydrogen bonding probably also begins between the clustered water molecules, and between these molecules and the "host" molecule. The ion charge is, of course, also present to complicate the intermolecular bond strengths. Whether a cluster thus formed can remain together after the ionic charge is neutralized is a question which will be addressed in the next section of this paper.

At the Chemical Systems Laboratory, extensive measurements also have been made of the electrical conductivity of moist air.[22, *]   A sharp dependence of ion content in water vapor upon temperature has been observed. For example, figure 18 shows the effect of

*Carlon, H.R. Ion Content of Air Humidified by Boiling Water. Submitted to J. Appl. Meterolol. (1978).

28
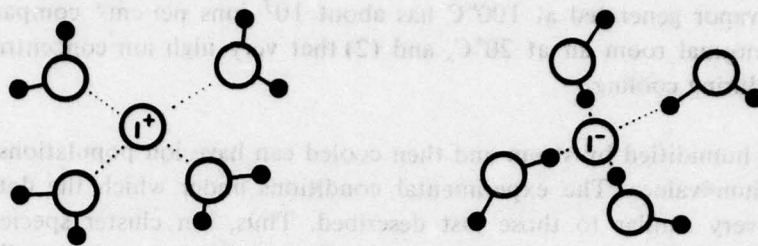
Figure 17. Water Ion Clusters (Ion Hydrates), c = 4
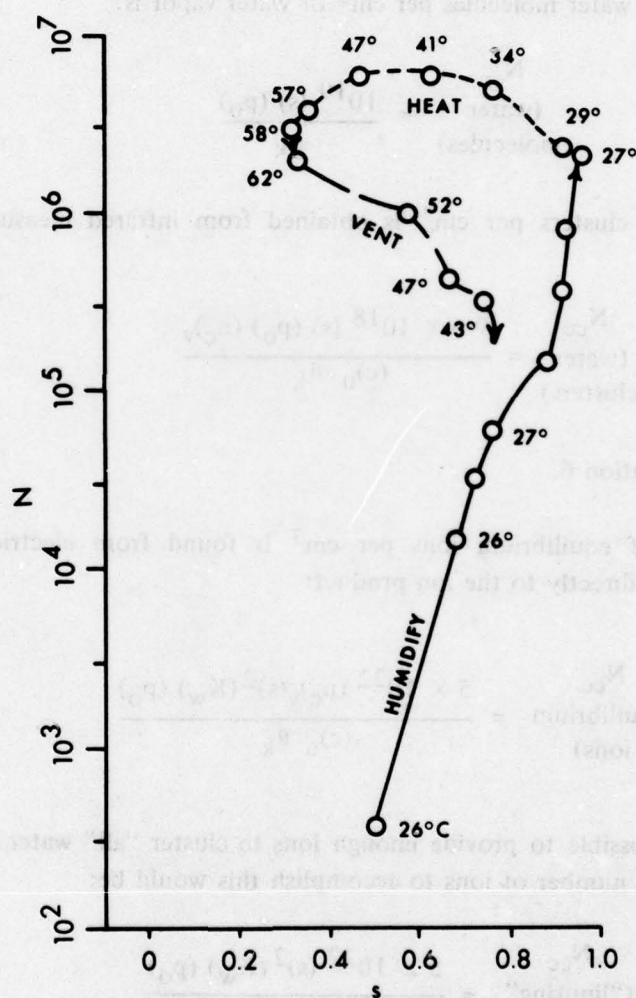
Figure 18. N, Ions per cm³ of Moist Air Humidified by Steam, Versus "s"

generating water vapor by boiling at 100°C, then cooling the vapor-saturated air to room temperature before measuring its electrical conductivity and, hence, its ion content. The results show (1) that water vapor generated at 100°C has about 10^7 ions per cm^3 compared to about 300 ions per cm^3 in normal room air at 20°C, and (2) that very high ion concentrations can be retained in moist air during cooling.

Thus, air humidified by steam and then cooled can have ion populations much larger than normal equilibrium values. The experimental conditions under which the data in figure 6 were obtained were very similar to those just described. Thus, ion cluster species could have contributed to the "bumps" in figure 6 which were observed to change repeatedly during the course of the measurements. And, these species could have contributed to luminescence-like activity which was also observed.[*]

The number of water molecules per cm^3 of water vapor is:

$$N_{cc} \atop \text{(water molecules)} \approx \frac{10^{19} (s) (p_O)}{\theta_k} \tag{15}$$

and the number of water clusters per cm^3 is obtained from infrared measurements already discussed:

$$N_{cc} \atop \text{(water clusters)} = \frac{9.6 \times 10^{18} (s) (p_O) (n_c)_v}{(c)_u \, \theta_k} \tag{16}$$

where $(n_c)_v$ is given by equation 6.

The number of equilibrium ions per cm^3 is found from electrical conductivity measurements to be related directly to the ion product:

$$N_{cc} \atop \text{(equilibrium ions)} = \frac{5 \times 10^{22} (n_c)_v (s)^2 (K_w) (p_O)}{(c)_u \, \theta_k} \tag{17}$$

And if it were somehow possible to provide enough ions to cluster "all" water molecules in the vapor ($I = 1$), the "limiting" number of ions to accomplish this would be:

$$N_{cc} \atop \text{("limiting" ions)} = \frac{5 \times 10^{22} (s)^2 (K_w) (p_O)}{(c)_u \, \theta_k} \tag{18}$$

---

[*] Carlon, H. R.   Variations in Emission Spectra from Warm Water Fogs: Evidence for Clusters in the Vapor Phase. Accepted for publication in Infrared Physics, approximately December (1978).

Equations 15-18 are summarized in figure 19, drawn for s = 1.0. This figure shows quite clearly the magnitude of the "discrepancy" between the number of ions per cm^3 and the number of water clusters per cm^3 required to account for the observed infrared absorption. Thus, if ions are involved directly in the formation of water clusters responsible for the infrared continuum absorption, they must necessarily play an intermediate role as discussed in the next section.
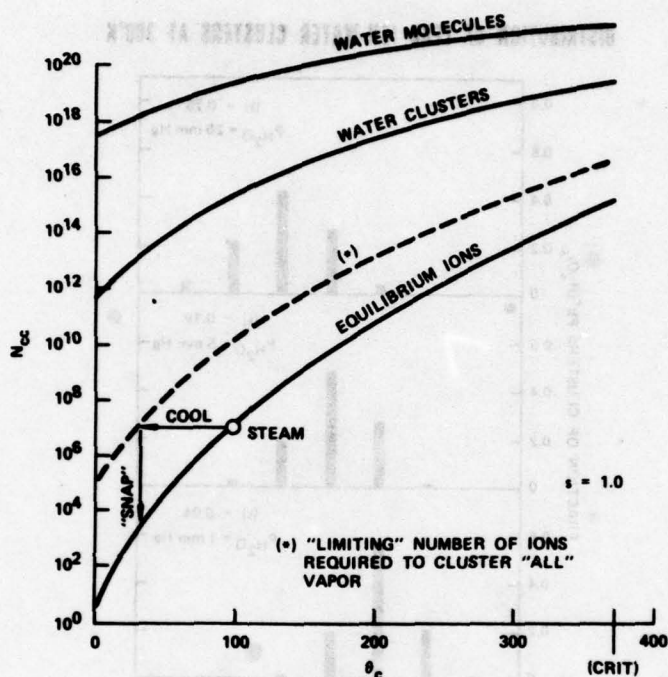
Figure 19. Plot of Equations 15 through 18

The small arrows in figure 19 indicate that cooling steam can contain enough ions to cluster (theoretically) "all" water vapor in moist air at room temperature. In actual fact, measurements* made under these conditions indicated that a few percent of the vapor was clustered (compared to only about 0.01 percent under normal equilibrium conditions). Thus, the fraction of total water vapor found in water clusters under these experimental conditions apparently was about the same as the fraction found as droplets in heavy, natural fogs.

Careful studies have actually been performed on some kinds of water ion clusters (ion hydrates). For example, the size distributions of Pb^+ clusters have been determined at 300°K for various values of s, the saturation ratio.[23,24] Although nothing is yet known about

---

*Carlon, H. R. Variations in Emission Spectra from Warm Water Fogs: Evidence for Clusters in the Vapor Phase. Accepted for publication in Infrared Physics, approximately December (1978).

31

the symmetry or bond geometries in such clusters, it can be seen in figure 20 that the mean (or modal) cluster size, $(c)_u$, varies directly with (s) according to:

$$(c)_u = k\ln(s) + K \tag{19}$$

Where K for Pb^+ water ion clusters is 6.2, and k is 0.68, for the data of figure 20.
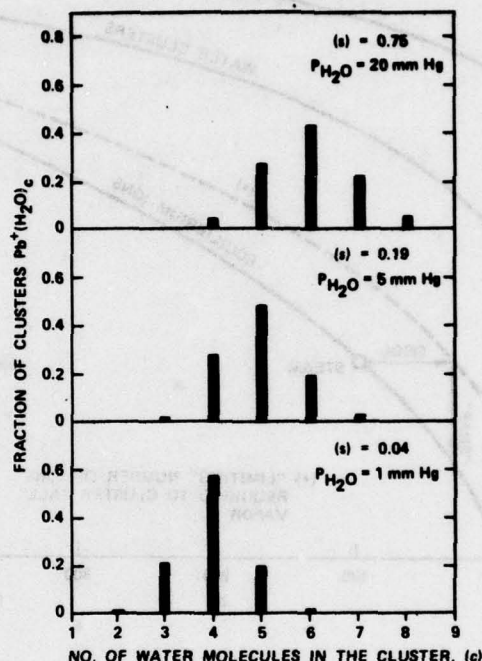
Figure 20. Data of Castleman and Tang (Reference 23)

For other ions than Pb^+, for example for the dissociative ions of water itself, the formation of clusters is easier and the constants k and K are larger. For example, at 300°K values of $k = 1.0$ and $K = 10$ are found to produce agreement between theory and measurement. Equation 19 can be used in a simple derivation with the Clausius-Clapeyron equation to yield:

$$(c)_u = k\left[\ln(p_W) + \frac{\Delta H}{R\theta_k} - 21\right] + K \tag{20}$$

where p_W is the water vapor partial pressure (sometimes also symbolized by "e"), and the assumption is made that the latent heat of vaporization of water also can be used to describe the temperature dependency of the cluster bond energy. Equation 20 is plotted in figure 21 for $k = 1.0$ and $K = 10$.

32
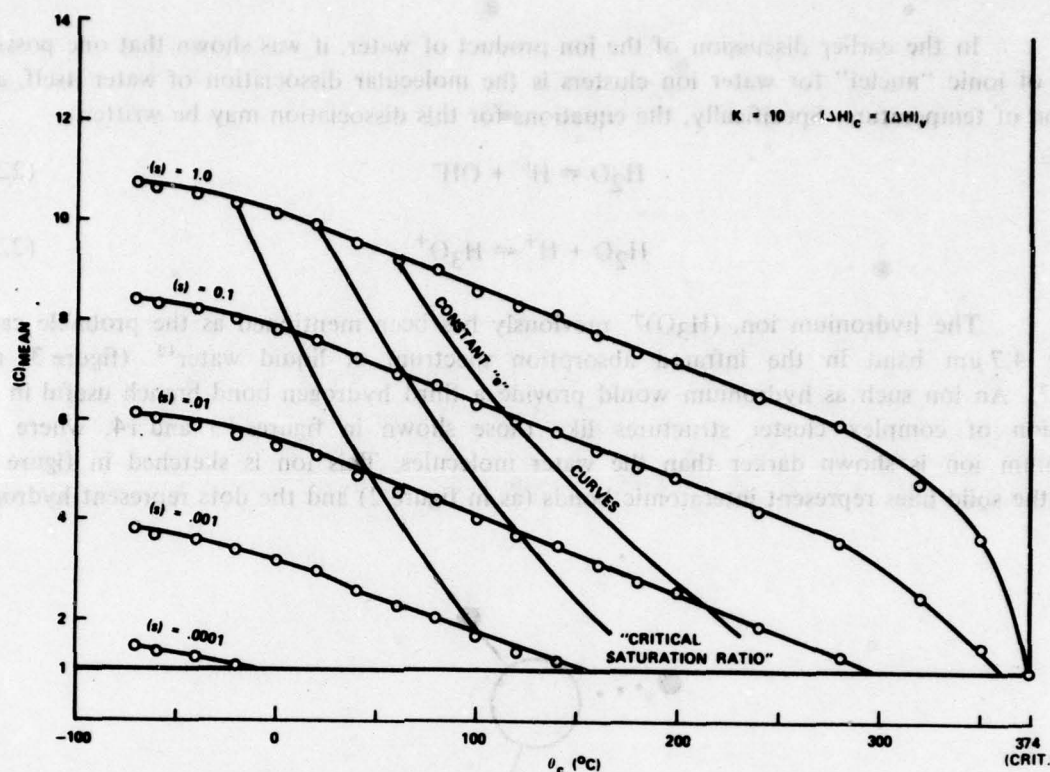
Figure 21. Equation 20, Plotted for k = 1.0 and K = 10

Equation 20 and figure 21 thus describe the expected mean size of an ion cluster distribution (for the constants specified), as a function of temperature and of saturation ratio. If the cluster distribution is known, and if the numbers and strengths of the intermolecular bonds in clusters of each size are known, then it is possible, in principle, to compute the infrared absorption spectrum of the distribution. In fact, the steam spectra of reference 5 (figure 5) and reference 11 (figure 6) show "bumps" which are distributed in wavelength as shown by equation 10. In figure 5, the spectral envelope appears to be "draped" over a distribution of absorption lines which lie at discrete wavelengths and, therefore, should be assignable to discrete cluster sizes given that the clusters are symmetrical, or at least given that most bonds in a given cluster have the same vibrational frequencies. On close inspection of the data, it is found that equation 10 fits the data if, and only if, the value of $K_V = 6.4$, so that: [5,14*]

$$\lambda_c = 6.4 \sqrt{c} \tag{21}$$

*Carlon, H. R. Variations in Emission Spectra from Warm Water Fogs: Evidence for Clusters in the Vapor Phase. Accepted for publication in Infrared Physics, approximately December (1978).

33

In the earlier discussion of the ion product of water, it was shown that one possible source of ionic "nuclei" for water ion clusters is the molecular dissociation of water itself, as a function of temperature. Specifically, the equations for this dissociation may be written:

$$H_2O \rightleftharpoons H^+ + OH^- \tag{22a}$$

$$H_2O + H^+ \rightleftharpoons H_3O^+ \tag{22b}$$

The hydronium ion, $(H_3O)^+$, previously has been mentioned as the probable cause of the $4.7\,\mu m$ band in the infrared absorption spectrum of liquid water[12] (figure 3, and figure 7). An ion such as hydronium would provide a third hydrogen bond branch useful in the formation of complex cluster structures like those shown in figures 13 and 14, where the hydronium ion is shown darker than the water molecules. This ion is sketched in figure 22, where the solid lines represent interatomic bonds (as in figure 2) and the dots represent hydrogen bonds.
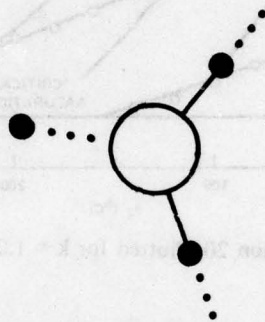
Figure 22. The Hydronium Ion

At least in the case of H_3O^+, the additional mass of a hydrogen atom has negligible effect upon the vibrational frequencies of hydrogen bonds in clusters which will be formed about it. There is also evidence that, once formed, a closed or ring-structured cluster can stay together without the ionic charge, due to its own intermolecular bonding. This will be discussed further in the next section. Certainly, in the liquid phase, water can be deionized without losing its identity or showing significant changes in its infrared spectrum. For finite lifetimes, perhaps the same thing can be said about clusters in the vapor phase.

Beginning with the hydronium ion, which could be considered an "ion cluster of size one",[25] a sequence of hydrogen ion water clusters can be proposed as shown in figure 23. In this figure, the dots again represent hydrogen bonds. A water molecule is added to the cluster between each step.

Interesting correlations begin to appear between cluster structures and the bond symmetry requirements implicit in equation 21. For example, the cluster of size 13 shown in figure 13 could have "grown" from a hydronium ion. From equation 9, this vapor phase cluster would have at least three different infrared-absorption wavelengths associated with it. But if the structure closes (figure 14) to form a lower energy ring configuration, equation 21 might be obeyed.

34
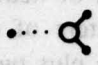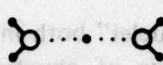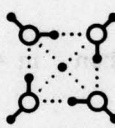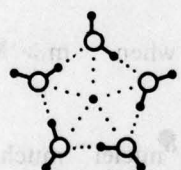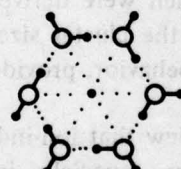
NAME	STRUCTURE	(c)	λ_c μm
HYDRONIUM		1	4.7
DIMER		2	9.1
TRIMER		3	11.1
QUATRAMER		4	12.8
PENTAMER		5	14.3
HEXAMER		6	15.7

Figure 23. A Possible Sequence of Water Ion Clusters
(λ_c is calculated from equation 21. The hydronium ion is
not symmetrical; hence equation 21 does not apply.)

C. Ion-Induced, Neutral Clusters.

When the formation of an ion cluster (ion hydrate), shown in equation 14 and figure 17, is followed by a charge neutralization event, an ion-induced, neutral cluster results. Such clusters can be formed by many different kinds of neutralization events, ranging from the simple loss of a charge to collisions between ion clusters of opposite charge, with the resulting cluster containing the sum of water molecules in both plus two molecules which previously were the ions in the respective clusters. The total number of water molecules in a new cluster (c), will be identical to that in other kinds of clusters, but the "nuclei" will be different.

Because of the added mass of ionic "nuclei" both in ion clusters and in ion-induced, neutral clusters, the simple empirical relationships of equation 10 and equation 21 become explicable as the "limiting" case of more complex oscillator models for larger cluster sizes. For example, it can be shown,*** that if "m" is the mass of the ion or neutral molecule cluster "nucleus", the resonant wavelengths are approximated by:

$$\lambda_c = K' \sqrt{(c-1)} \quad \text{when} \quad m \approx 0 \tag{23}$$

$$\lambda_c = K'' \sqrt{\frac{c^2}{c+1}} \quad \text{when} \quad m \approx M \tag{24}$$

$$\lambda_c = K''' \sqrt{c} \quad \text{when} \quad m \gg M \tag{25}$$

Thus the form of equation 25 (for "nuclei" much heavier than water molecules) already has the form of equations 10 and 21 (which were derived from empirical observations), while equations 23 and 24 approach this form as the cluster size (c) increases. In effect, clusters of almost any mass should exhibit this $\lambda_c = K\sqrt{c}$ behavior, provided that $(c) \gg 1$.

Experimental evidence supports the view that ion-induced, neutral water clusters can have lifetimes which may reach an hour or more, especially in saturated water vapor. This is thought to happen because intermolecular bonds (including hydrogen bonds) which "cross-link" a cluster during its formation about an ion are able to hold it, or a larger cluster, together even if a collision of two clusters occurs. Thus, the size distribution already discussed for ion clusters like Pb^+ hydrates may also represent those of ion-induced, neutral clusters, and the latter could be present in sufficient numbers to explain the infrared continuum absorption. This would also explain the functional correlation between infrared absorption and electrical conductivity (ion content) of moist air, while at the same time removing the "discrepancy" between the required numbers of water clusters and the numbers of short-lived equilibrium ions producing them (figure 19).

*Carlon, H.R. A Molecular-Cluster (Ion Hydrate) Explanation of the Infrared Water Vapor Continuum Absorption. Submitted to J. Opt. Soc. Am. (1978).

**Carlon, H.R. Empirical Evidence for Clustered Molecules in Water Vapor. Submitted to Applied Optics (1978).

Many papers have appeared in recent years addressing topics related to vibrational frequencies and force constants of water clusters[26,27] and liquid water,[28] ion clusters (ion hydrates)[23,24,29] and molecular processes in nucleation.[30]

VI. CLUSTER-SIZE DISTRIBUTIONS.

The homogeneous cluster distribution is dominated by the dimer, and is thought to look about as shown in figure 24, for water vapor at 20°C, "s" = 1.0:
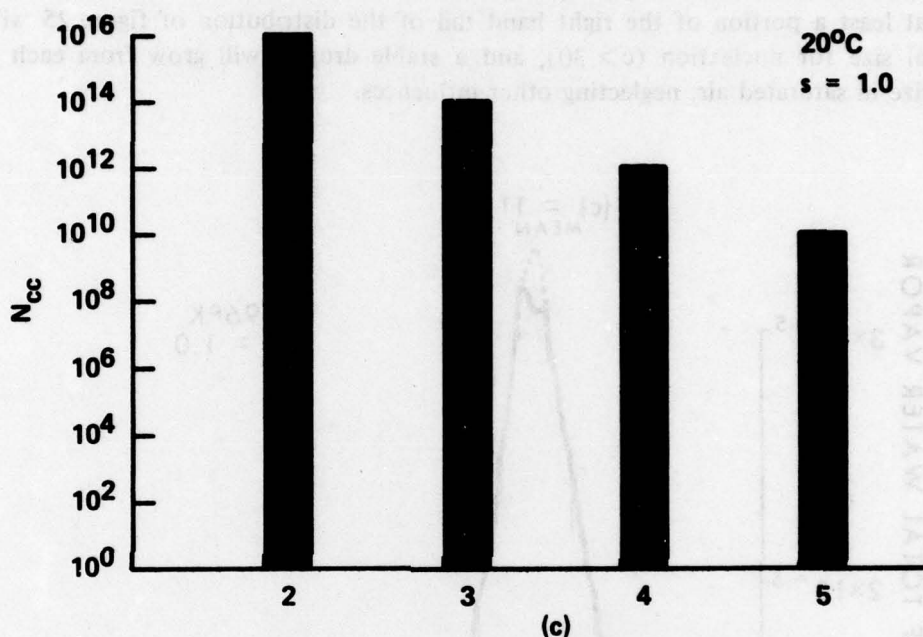
Figure 24. Number Distribution of Homogeneous Clusters

Homogeneous clusters larger than the dimer are present in such small numbers that they should have a vanishingly small influence on the infrared continuum absorption spectrum of water vapor. Thus, the dimer would have to "explain" observed spectra by itself, in the absence of ion-induced, neutral clusters. The predicted vibrational frequencies for the dimer, however, do not agree with experimental observations.* Hence, the dimer is probably only a contributor to the continuum absorption spectrum due to distributions of larger clusters.

Based upon electrical conductivity measurements of moist air, ion clusters (ion hydrates) are not present in nearly sufficient numbers to account for observed absorption. But the neutral clusters which they induce could be present in sufficient numbers to explain all experimental observations. The balance of this discussion will deal with such distributions.

---

*Carlon, H.R.   Molecular Interpretation of the ir Water Vapor Continuum: Comments. Accepted for publication in Applied Optics 17 (1978).

If k = 1.0 and K = 10 in equation 20, the mean cluster size $(c)_u$ at 23°C (s = 1.0) is found to be 10. From equations presented earlier, assuming approximate symmetry about $(c)_u$, the distributions of figure 25 are calculated for ion-induced, neutral clusters. The lower curve (for s = 1.0) is compared to an upper curve for a supersaturation of s = 4.2, which is the value required under normal ambient starting conditions to nucleate liquid water droplets in a cloud chamber.[31]

Note that increasing "s" not only increases the mean value of cluster size, $(c)_u$, according to equation 20, but it also increases the mass fraction of water vapor which is clustered (equation 6). This insures that by the time that the supersaturation approaches the critical level, at least a portion of the right hand tail of the distribution of figure 25 will have attained critical size for nucleation (c > 30), and a stable droplet will grow from each cluster attaining this size in saturated air, neglecting other influences.
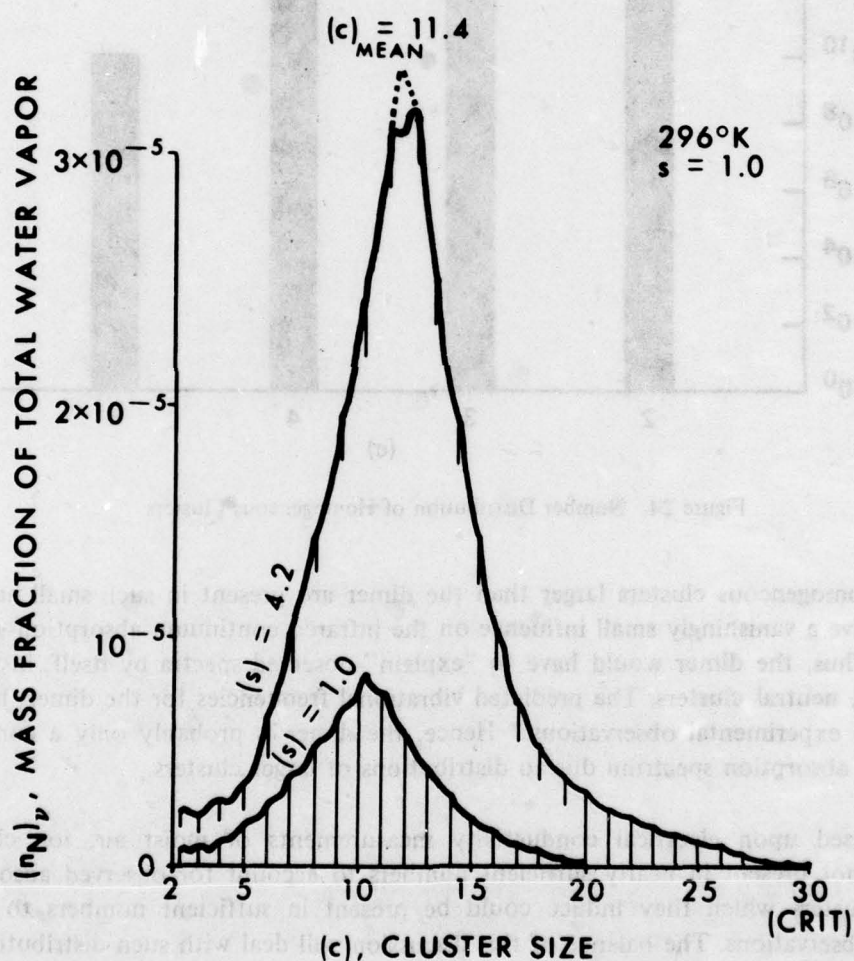
Figure 25. Distribution of Ion-Induced, Neutral Clusters by Mass Fraction
of Total Water Vapor

The cluster number distribution can be obtained simply by rewriting equation 16 for each cluster size:

$$\frac{(N_N)_{cc}}{\text{(water clusters)}} = \frac{9.6 \times 10^{18} \, (s) \, (p_o) \, (n_N)_v}{(c)_N \, \theta_k} \tag{26}$$

Equation 26 is plotted in figure 26. A contribution is included in the figure for the homogeneous dimer and trimer (figure 24) as a reminder that these cluster species may play a role (perhaps a significant role) in the infrared continuum absorption.
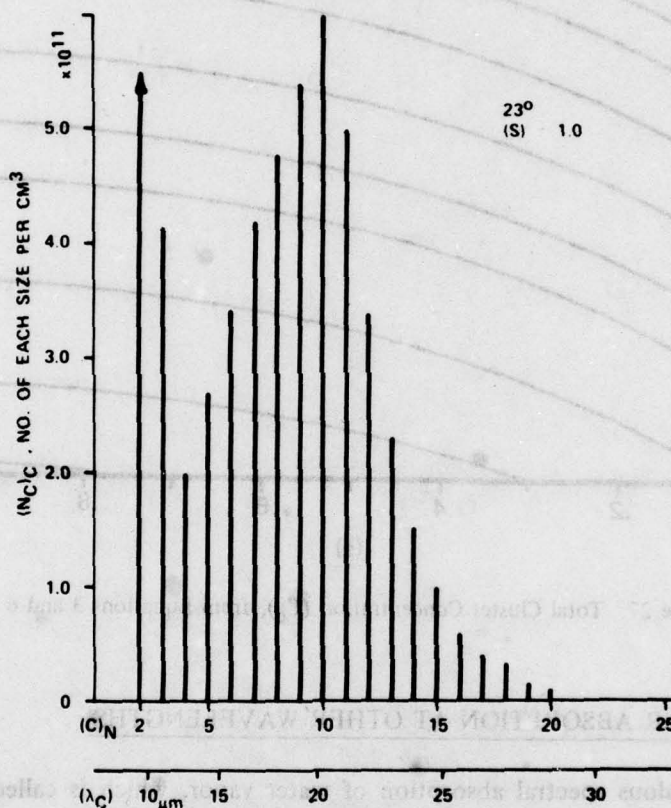
Figure 26. Cluster Number Distribution (Equation 26)
(λ_c also is shown, from equation 21.)

It is also useful to plot, for reference purposes, the total concentrations of water clusters which are present in moist air at various temperatures and saturation ratios (equation 3), as shown in figure 27. $(n_c)_v$ was evaluated from equation 6 (figure 10).

39
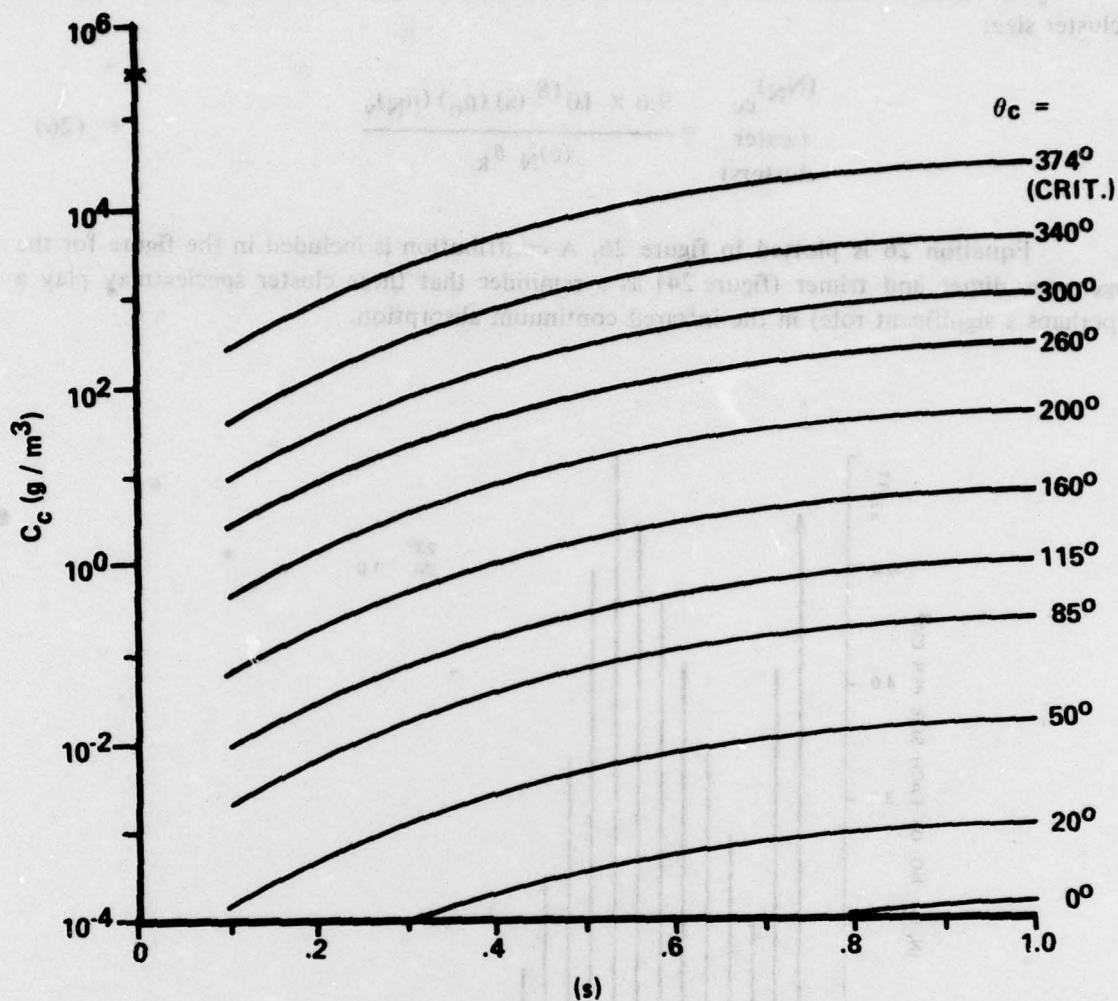
Figure 27. Total Cluster Concentration (C_c), from Equations 3 and 6

VII. WATER CLUSTER ABSORPTION AT OTHER WAVELENGTHS.

The anomalous spectral absorption of water vapor, which is called the "continuum absorption" in the infrared, apparently is not limited only to these shorter wavelengths. While a true continuum of absorption does not exist with increasing wavelength out to the microwave region, spectral intervals are found where absorption attributed to water clusters (especially to the dimer) has been found.[20] Many measurements have been made[32,33] in the region from 4 cm^{-1} to 32 cm^{-1}, where results indicate that at low temperatures the observed levels of anomalous atmospheric absorption cannot be attributed to water dimers in equilibrium.[33]

40

There is a simple test* to measure the tendency of a substance to form spectrally absorbing intermolecular bonds (i.e., to cluster), which works very well for water in the 8-13 μm region:

> *If, at some wavelength, the measured molecular absorption coefficient of a liquid (e.g., water) is found to be substantially larger than this coefficient for the liquid's vapor phase, this is prima facie evidence that intermolecular bonding (clustering) exists within the samples and that the intermolecular bonds are active in the absorption at the measurement wavelength.*

When this test is applied at longer wavelengths, it predicts water cluster absorption levels which agree reasonably well with observed results. The test ratio of molecular absorption coefficients for liquid water and water vapor at wavelength λ, $(\alpha_\ell/\alpha_v)_\lambda$, is shown as a function of wavelength in figure 28, for 20°C and "s" = 0.43.
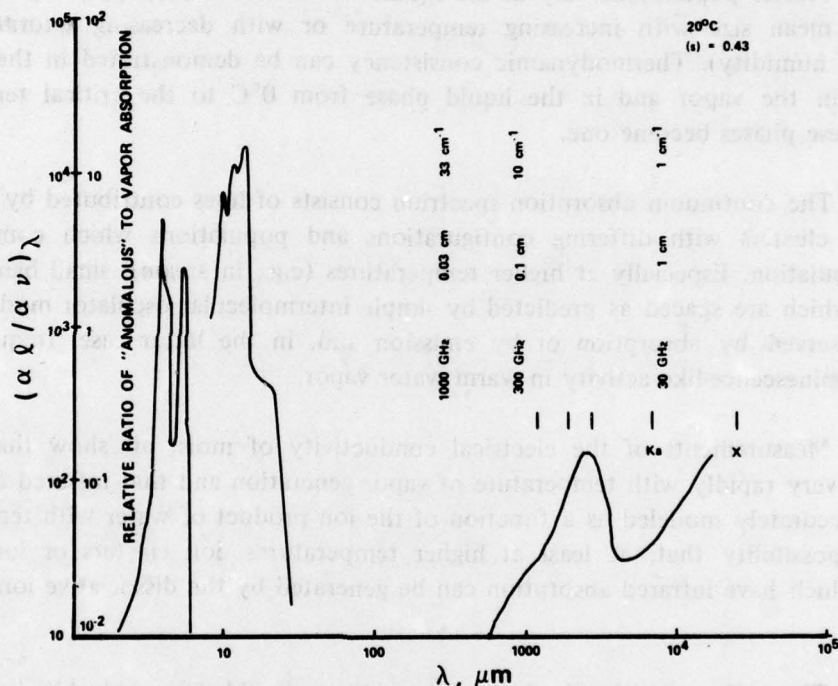
Figure 28. Ratio of Molecular Absorption Coefficients for Liquid Water and Water Vapor, Versus Wavelength

The amplitude of the curve is greatest in the 8-13 μm region, where greatest anomalous absorption is observed, and the curve is lower by an average of about 10 to 20 times in the 3-5 μm region, again agreeing well with experimental data. In the 4 cm⁻¹ to 32 cm⁻¹ region (centered near 1000 μm), figure 28 shows levels of predicted anomalous absorption averaging perhaps a decade below those in the 3-5 μm region, but rising at longer wavelengths (near 4 cm⁻¹), where they approximate those in the 3-5 μm "window".

---

*Carlon, H. R.   Phase Transition Changes in the Molecular Absorption Coefficient of Water in the Infrared: Evidence for Clusters.   Accepted for publication in Applied Optics *17* (1978).

VIII. CONCLUSIONS:

The development presented in this paper leads to the following principal conclusions:

1. The infrared continuum absorption of water "vapor" can be explained as the absorption due to intermolecular bonds in "liquid-like" clusters of water molecules which are present in fractions of about 10^{-4} to 10^{-3} in the vapor phase.

2. The water species responsible for the continuum absorption can be homogeneous, and limited to a few molecules (like the dimer). Or, their populations can have mean sizes of about 10 molecules and can range in size from a few molecules to 30 or more molecules. The latter kinds include ion clusters (ion hydrates) and ion-induced, neutral clusters.

3. Cluster populations vary as the square of the water vapor partial pressure, and they decrease in mean size with increasing temperature or with decreasing saturation ratio (fractional relative humidity). Thermodynamic consistency can be demonstrated in the behavior of clusters both in the vapor and in the liquid phase from 0°C to the critical temperature (374°C), where these phases become one.

4. The continuum absorption spectrum consists of lines contributed by modes of various bonds in clusters with differing configurations and populations which comprise the overall cluster population. Especially at higher temperatures (e.g., in steam), small bands appear in the spectrum which are spaced as predicted by simple intermolecular oscillator models. These bands can be observed by absorption or by emission and, in the latter case, frequently are associated with luminescence-like activity in warm water vapor.

5. Measurements of the electrical conductivity of moist air show that the ion content increases very rapidly with temperature of vapor generation and that infrared absorption can, in fact, be accurately modeled as a function of the ion product of water with temperature. This allows the possibility that, at least at higher temperatures, ion clusters or ion-induced, neutral clusters which have infrared absorption can be generated by the dissociative ionization of water, itself.

6. Thus, the nature of cluster absorption should be resolvable in carefully designed experiments to measure continuum absorption in a multipass optical cell, in the presence of an electrical field which can be varied with time, where the water vapor is generated at controlled temperatures and by different techniques.

7. The anomalous spectral absorption of water vapor which is called the "continuum absorption" in the infrared, apparently is not limited only to these shorter wavelengths. While a true continuum does not exist with increasing wavelength out to the microwave region, spectral intervals are found where absorption attributed to water clusters has been found. For example, the absorption near 4 cm^{-1} can approximate the continuum absorption in the 3-5 μm "window".

42

LITERATURE CITED

1.   Carlon, H.R.   The Apparent Dependence of Terrestrial Scintillation Intensity Upon Atmospheric Humidity. Applied Optics 4, 1089-1097 (1965).

2.   Papers of Luck, W.A.P.   Summarized in Franks, F. ed., "Water: A Comprehensive Treatise- Vol. 1", p. 210 ff. Plenum Press, New York (1972).

3.   Carlon, H.R.   Humidity Effects in the 8-13μ Infrared Window. Applied Optics 5, 879 (1966).

4.   Carlon, H.R.   Infrared Emission By Fine Water Aerosols and Fogs. Applied Optics 9, 2000-2006 (1970).

5.   Varanasi, P., Chou, S., and Penner, S.S.   Absorption Coefficients for Water Vapor in the 600-1000 cm^{-1} Region. J. Quant. Spectrosc. Radiat. Transfer 8, 1537-1541 (1968).

6.   Carlon, H.R.   Model for Infrared Emission of Water Vapor/Aerosol Mixtures. Applied Optics 10, 2297-2303 (1971).

7.   Burroughs, W.J. Jones, R.G., and Gebbie, H.A.   Study of Submillimeter Atmospheric Absorption Using the Hydrogen Cyanide Laser. J. Quant. Spectrosc. Radiat. Transfer 9, 809-824 (1969).

8.   Bignell, K.J.   The Water-Vapor Infra-Red Continuum. Q.J.R. Meteorol. Soc. 96, 390-403 (1970).

9.   Penner, S.S.   Effect of Dimerization on the Transmission of Water Vapor in the Near Infrared. J. Quant. Spectrosc. Radiat. Transfer 13, 383-384 (1973).

10.   Carlon, H.R.   ARCSL-TR-78001.   Anomalous Infrared Emission from Condensing and Cooling Steam Clouds. Aberdeen Proving Ground, MD 21010.   December 1977

11.   Hale, G.M., and Querry, M.R.   Optical Constants of Water in the 200-nm, to 200μm Wavelength Region.   Applied Optics 12, 555-563 (1973).

12.   Falk, M., and Giguere, P.A.   Infrared Spectrum of the H_3O^+ Ion in Aqueous Solutions. Can. J. Chem. 35, 1195-1204 (1957).

13.   Pinkley, L.W., Sethna, P.P., and Williams, D.   The Influence of Cupric Ions on the Infrared Spectrum of Water.   J. Opt. Soc. Am. 67, 494 (1977).

14.   Frank, H.S., and Wen, W.Y.   Structural Aspects of Ion-Solvent Intereaction in Aqueous Solution – A Suggested Picture of Water Structure. Discuss. Faraday Soc. 24, 133-143 (1957).

15.   Roberts, R.E., Selby, J.E.A., and Biberman, L.M.   Infrared Continuum Absorption by Atmospheric Water Vapor in the 8-12μm Window.   Applied Optics *15*, 2085-2090 (1976).

16.   Carlon, H.R.   ARCSL-TR-78014.   Introduction to Polymolecular Water Clusters and Their Infrared Activity.   Aberdeen Proving Ground, MD 21010, February 1978.

17.   Montgomery, G.P.,Jr.   Temperature Dependence of Infrared Absorption by the Water Vapor Continuum near 1200 cm^{-1}.   Applied Optics *17*, 2299-2303 (1978).

18.   Carlon, H.R.   ARCSL-TR-77059.   Infrared Absorption Spectra Attributed to Ion-Nucleated Water Clusters.   Aberdeen Proving Ground, MD 21010,   September 1977.

19.   Wolynes, P.G. and Roberts, R.E.   Molecular Interpretation of the Infrared Water Vapor Continuum.   Applied Optics *17*, 1484-1486 (1978).

20.   Jones, D.T. Llewellyn, Knight, R.J., and Gebbie, H.A.   Absorption by Water Vapour at 7.1 cm^{-1} and its Temperature Dependence.   Nature (London) *274*, 876-878 (31 August 1978).

21.   Papers of Holzapfel, W. summarized in F. Franks, ed.,   "Water: A Comprehensive Treatise- Vol. 1", p. 503 ff, Plenum Press, New York (1972).

22.   Carlon, H.R.   ARCSL-TR-78007.   Electrical Conductivity of Moist Air I: Cell Design and Fabrication From the Water Cluster Theory.   Aberdeen Proving Ground, MD 21010, May 1978.

23.   Castleman, A.W., Jr., and Tang, I.N.   Role of Small Clusters in Nucleation About Ions.   J. Chem. Phys. *57*, 3629-3638 (1972).

24.   Castleman, A.W., Jr.,   Nucleation Processes and Aerosol Chemistry.   Space Sci. Rev. *15*, 547 (1974).

25.   Newton, M.D.   AbInitio Studies on the Hydrated Hydronium H$_3$O$^+$) ion. II. The Energetics of Proton Motion in Higher Hydrates (n = 3-5).   J. Chem. Phys. *67*(12), 5535-5546 (1977).

26.   Curtis, L.A., and Pople, J.A.   AbInitio Calculation of the Vibrational Force Field of the Water Dimer.   J. Mol. Spectrosc. *55*(1-3) 1-14, (1975).

27.   Owicki, J.C., Shipman, L.L., and Scheraga, H.A.   Structure, Energetics and Dynamics of Small Water Clusters.   J. Phys. Chem. *79*(17), 1794-1811 (1975).

28.   Stillinger, F.H., and Rahman, A.   Improved Simulation of Liquid Water by Molecular Dynamics.   J. Chem. Phys. *60*(4), 1545-1557 (1974).

29.   Castleman, A.W., Jr., Holland, P.M., and Keesee, R.G.   The Properties of Ion Clusters and Their Relationship to Heteromolecular Nucleation.   J. Chem. Phys. *68*(4), 1760-1767 (15 February 1978).

30.   Hale, B.N., and Plummer, P.L.M.   Nucleation Phenomena. I. Molecular Model. J. Atmos. Sci. *31*(6), 1615-1621 (1974).

31.   Work of Wilson, C.T.R. as summarized by Wilson, J.G. in The Principles of Cloud-Chamber Technique. Cambridge, The University Press (1951).

32.   Emery, R.J., Moffat, P., Bohlander, R.A., and Gebbie, H.A.   Measurements of Anomalous Atmospheric Absorption in the Wavenumber Range $4 \text{ cm}^{-1} - 15 \text{ cm}^{-1}$.   J. Atmos. and Terres. Phys. *37*, 587-594 (1975).

33.   Gimmestad, G.G., and Gebbie, H.A.   Atmospheric Absorption in the Range 12 cm^{-1} to 32 cm^{-1} Measured in Horizontal Path.   J. Atmos. and Terr. Phys. *38*, 325-328 (1976).

Names	Copies	Names	Copies

CHEMICAL SYSTEMS LABORATORY

SAFETY OFFICE
Attn: DRDAR-CLF

PLANNING & TECHNOLOGY OFFICE
Attn: DRDAR-CLR-L ... 1

AUTHOR'S COPIES: Research Division ... 50

BIOMEDICAL LABORATORY
Attn: DRDAR-CLL-B
Attn: DRDAR-CLL-MC ... 1

CB DETECTION & ALARMS DIVISION
Attn: DRDAR-CLC-C ... 1

DEVELOPMENTAL SUPPORT DIVISION
Attn: DRDAR-CLJ-R ... 3
Attn: DRDAR-CLJ-L ... 3

ENVIRONMENTAL TECHNOLOGY DIVISION
Attn: DRDAR-CLT-E ... 1

MUNITIONS DIVISION
Attn: DRDAR-CLN ... 1

PHYSICAL PROTECTION DIVISION
Attn: DRDAR-CLW-P ... 1

RESEARCH DIVISION
Attn: DRDAR-CLB ... 1
Attn: DRDAR-CLB-B ... 1
Attn: DRDAR-CLB-C ... 1
Attn: DRDAR-CLB-P ... 1
Attn: DRDAR-CLB-R ... 1
Attn: DRDAR-CLB-T ... 1
Attn: DRDAR-CLB-TE ... 1

SYSTEMS ASSESSMENTS OFFICE
Attn: DRDAR-CLY ... 1
Attn: DRDAR-CLY-R ... 1

DEPARTMENT OF DEFENSE

Administrator
Defense Documentation Center
Attn: Document Processing Division (DDC-DD) ... 2
Cameron Station
Alexandria, VA 22314

Director
Defense Intelligence Agency
Attn: DB-4G1 ... 1
Washington, DC 20301

DEPARTMENT OF THE ARMY

HQDA (DAMO-SSC) ... 1
WASH DC 20310

Deputy Chief of Staff for Research,
Development & Acquisition
Attn: DAMA-CSM-CM ... 1
Attn: DAMA-ARZ-D ... 1
Washington, DC 20310

US Army Research and Standardization
Group (Europe)
Attn: Chief, Chemistry Branch
Box 65, FPO New York 09510

Commander
HQ US Army Medical Command, Europe
Attn: AEMPM ... 1
APO New York 09403

US ARMY MATERIEL DEVELOPMENT AND READINESS COMMAND

Commander
US Army Materiel Development and Readiness Command
Attn: DRCLDC ... 1
Attn: DRCSF-P ... 1
5001 Eisenhower Ave
Alexandria, VA 22333

Commander
US Army Toxic and Hazardous Materials Agency
Attn: DRXTH-TS ... 2
Aberdeen Proving Ground, MD 21010

Project Manager Smoke/Obscurance
Attn: DRCPM-SMK-M ... 1
Aberdeen Proving Ground, MD 21005

Human Engineering Laboratory HFE Detachment
ATTN: DRXHE-EA ... 1
Building E3220
Aberdeen Proving Ground, MD 21010

US Army Materiel Systems Analysis Activity
Attn: DRXSY-MP ... 1
Attn: DRXSY-T (Mr. Kaste) ... 1
Aberdeen Proving Ground, MD 21005

Commander
US Army Missile Research and Development Command
Redstone Scientific Information Center
Attn: DRDMI-TBD ... 1
Redstone Arsenal, AL 35809

Director
DARCOM Field Safety Activity
Attn: DRXOS-C ... 1
Charlestown, IN 47111

Names	Copies

US ARMY ARMAMENT RESEARCH AND DEVELOPMENT COMMAND

Commander
US Army Armament Research and Development Command
   Attn: DRDAR-LCA   1
   Attn: DRDAR-LCE   2
   Attn: DRDAR-LCE-M   1
   Attn: DRDAR-LCF   1
   Attn: DRDAR-LCU   1
   Attn: DRDAR-SCA-PP   1
   Attn: DRDAR-SCN   1
   Attn: DRDAR-SCP-A   1
   Attn: DRDAR-SER   1
   Attn: DRDAR-TSS   2
Dover, NJ 07801

Director
Ballistic Research Laboratory
   Attn: DRDAR-TSB-S   1
Building 305
Aberdeen Proving Ground, MD 21005

CDR, APG
USA ARRADCOM
   Attn: DRDAR-GCL   1
Aberdeen Proving Ground, MD 21010

US ARMY ARMAMENT MATERIEL READINESS COMMAND

Commander
US Army Armament Materiel Readiness Command
   Attn: DRSAR-ASN   1
   Attn: DRSAR-IRB   1
Rock Island, IL 61201

Commander
US Army Dugway Proving Ground
   Attn: Technical Library, Docu Sect
Dugway, UT 84022

Commander
Rocky Mountain Arsenal
   Attn: SARRM-QA   1
Commerce City, CO 80022

Commander
Pine Bluff Arsenal
   Attn: SARPB-ETA   1
Pine Bluff, AR 71611

US ARMY TRAINING & DOCTRINE COMMAND

Commandant
US Army Infantry School
   Attn: NBC Division   1
Fort Benning, GA 31905

Names	Copies

Commandant
US Army Military Police School/Training Center
   Attn: ATZN-TDP-C   1
Fort McClellan, AL 36205

Commander
US Army Infantry Center
   Attn: ATSH-CD-MS-C   1
Fort Benning, GA 31905

DEPARTMENT OF THE NAVY

Chief of Naval Research
   Attn: Code 443   1
800 N. Quincy Street
Arlington, VA 22217

Commanding Officer
Naval Weapons Support Center
   Attn: Code 5042/Dr. B. E. Douda   1
Crane, IN 47522

DEPARTMENT OF THE AIR FORCE

HQ Foreign Technology Division (AFSC)
   Attn: PDRR   1
Wright-Patterson AFB, OH 45433

Commander
Aeronautical Systems Division
   Attn: ASD/AELD   1
Wright-Patterson AFB, OH 45433

HQ AFISC/SEV   1
Norton AFB, CA 92409

OUTSIDE AGENCIES

Battelle, Columbus Laboratories
   Attn: TACTEC   1
505 King Avenue
Columbus, OH 43201

Director of Toxicology   1
National Research Council
2101 Constitution Ave, NW
Washington, DC 20418

Director
Central Intelligence Agency
   Attn: ORD/DD/S&T   1
Washington, DC 20505

ADDITIONAL ADDRESSEES

Commander
USEUCOM
   Attn: ECJ5-0/LTC James H. Alley
APO, NY 09128

Names	Copies	Names	Copies
US Public Health Service Room 17A-46 (CPT Osheroff) 5600 Fishers Lane Rockville, MD 20857	1	USA Atmospheric Sciences Laboratory DRSEL-BL-AS-P (Dr. K. White) White Sands Missile Range, NM 88002	1
Commander US Army Environmental Hygiene Agency Attn: Librarian, Bldg 2100 Aberdeen Proving Ground, MD 21010	1	Dr. John N. Howard 7 Norman Road Newton Highlands, MA 02161	1
Commander DARCOM, STITEUR Attn: DRXST-ST1 Box 48, APO New York 09710	1	Commander USA Research Office Box 12211 DRXRO-GS (Attn: Dr. A. Dodd) Research Triangle Park, NC 27709	1
Dr. James L. Kassner, Director Graduate Center for Cloud Physics Space Sciences Research Center University of Missouri-Rolla Rolla, Missouri 65401	1	Dr. Darrell Burch Aeroneutronic Division Ford Aerospace and Communications Ford Road Newport Beach, CA 92663	1
HQDA Attn: DAMA-ARZ-D (Dr. F. Verderame) Washington, DC 20310	1	Dr. Mark Sharnoff Dept of Physics Univ of Delaware Newark, DE 19711	1
Prof. Marvin R. Querry Dept. of Physics University of Missouri Kansas City, MO 64110	1	USA Rsch & Standardization Group (Europe) Attn: Dr. Hoyt Lemons Box 65, FPO New York 09510	1
Dr. Raymond Mackay Dept of Chemistry Drexel University 32nd & Chesnut Streets Philadelphia, PA 19104	1	Dr. D. Deirmendjian The Rand Corporation Main Street Santa Monica, CA 90406	1
AFGL/OPI/Stop 30 Attn: Dr. R. McClatchey Hanscom AFB, MA 01731	1	Dr. Robert Meredith Science Applications, Inc. 15 Research Drive Ann Arbor, Michigan 48103	1
Prof. Ronald K. Long Ohio State Univ. Research Foundation 1314 Kinnear Road Columbus, Ohio 43212	1	Prof. Benjamin M. Herman Inst. of Atmospheric Physics Univ. of Arizona Tucson, Arizona 85721	1
Dr. Robert E. Roberts Inst. for Defense Analysis Science & Technology Division 400 Army-Navy Drive Arlington, VA 22202	1	Dr. Robert Spellicy Science Applications, Inc. % Atmospheric Sciences Laboratory DRSEL-BL-AS-P (Attn: K. White) White Sands Missile Range, NM 88002	1
Dr. James J. Gallagher Engineering Experiment Station Georgia Inst. of Technology Atlanta, GA 30332	1	Dr. R.W. Terhune, Editor OPTICS LETTERS Ford Motor Co. Research Labs P.O. Box 2053 Dearborn, Michigan 48121	1
USA Ballistic Research Laboratory DRDAR-BLB (Dr. Geo. Keller) Aberdeen Proving Ground, MD 21005	1	Armament Concepts Office, Weapons Systems Concepts Team Attn: DRDAR-ACW Aberdeen Proving Ground, MD 21010	1